

MECHANISM OF INTERACTION  
OF GRAPHITE OXIDE AND AMMONIA VAPOR

by

BERNARD CARL SEILER

A THESIS

submitted to

OREGON STATE UNIVERSITY

in partial fulfillment of  
the requirements for the  
degree of

DOCTOR OF PHILOSOPHY

June 1962

APPROVED:

[REDACTED]

Professor of Chemistry

[REDACTED]

Chairman of Department of Chemistry

[REDACTED]

Chairman of School Graduate Committee

[REDACTED]

Dean of Graduate School

Date thesis is presented August 4, 1961

Typed by LeAnna Harris

#### ACKNOWLEDGEMENT

The author thanks the National Science Foundation for the grant in aid which made this study possible. He is most grateful to Professor W.H. Slabaugh for his encouragement, patience, suggestions, and assistance in the experimental work and interpretation of results. Also, thanks is given to M.E. Harward and A. Theisen of the Agricultural Department for their assistance in obtaining the X-ray diffraction data.

## TABLE OF CONTENTS

	Page
INTRODUCTION	1
Scope of Problem	1
History of Graphite Oxide	3
Physical Properties	5
Chemical Properties	7
Composition and Structure	12
Adsorption of Vapors and Gases	19
THEORETICAL BACKGROUND	24
Adsorption	24
Heats of Adsorption	30
Infrared Absorption	34
X-Ray Diffraction	37
EXPERIMENTAL PROCEDURES	38
Sample Preparation	38
Absorption Apparatus and Procedure	45
Infrared Absorption	51
X-ray Diffraction	55
Measurement of Heats of Adsorption	59
DISCUSSION OF EXPERIMENTAL RESULTS	67
Adsorption Isotherms	67
Adsorption Isobars	78
Infrared Absorption	83
X-ray	89
Heats of Adsorption	98
Summary of Adsorption Mechanism	104
FURTHER INVESTIGATION SUGGESTED BY THIS STUDY	106
Adsorption Studies	106
Miscellaneous Studies	106
SUMMARY	108
BIBLIOGRAPHY	110

LIST OF TABLES

	Page
Table I	
A. Composition of Graphite Oxide	
B. Concentration of Metal in Graphite Oxide	43
Table II. Summary of Adsorption Behavior of Graphite Oxides and Salts	71

# MECHANISM OF INTERACTION OF GRAPHITE OXIDE AND AMMONIA VAPOR

## INTRODUCTION

### Scope of Problem

Although graphite oxide has been known since Brodie (13,p.249-259) first oxidized graphite with fuming nitric acid and potassium chlorate, little has been reported about its gas adsorption properties.

Graphite oxide has two features which make it a potentially good adsorbate. First, graphite oxide retains a laminar structure similar in some respects to graphite itself (63,p.43-56), and therefore it should have approximately the same surface area as graphite. Second, graphite oxide has been found by Thiele (74,p.1-20)(73,p.167-168)(75,p.144-153), Hoffman (47,p.311-336) and others to have radicals such as carboxyl, hydroxyl, epoxy and possibly peroxy groups attached to the graphite hexagonal platelets. These groups constitute energetic sites for chemical adsorption, especially for polar molecules.

The adsorption of water and certain non-polar gases such as nitrogen and hexane on graphite oxide has been studied by a number of investigators (11,

p.242-252)(67,p.453-455). They found that, while there was considerable water adsorption, the adsorption of non-polar gases was small in comparison. The high adsorption of water is attributed to the intercalation of water molecules between the graphite oxide platelets, which is possible because of the high dipole moment of water and the hydrophilic nature of graphite oxide.

Since graphite oxide has acidic properties, the adsorption of a basic molecule such as ammonia should even be more pronounced. Also, while the dipole moment is smaller than water,  $\text{NH}_3$  is more polarizable in the presence of polarizing groups as found in the oxide. These two factors tend to make ammonia an ideal gas with which to advance the studies of the surface properties and even the structure of graphite oxide.

The present work shows the results of such an investigation with ammonia involving adsorption isotherms, x-ray, infrared, and heats of adsorption studies. Proposals for the mechanism of interaction of ammonia with graphite oxide are also included in this work. It is hoped that this investigation has helped elucidate the structure and nature of graphite oxide surfaces.

### History of Graphite Oxide

Graphite oxide or graphitic acid was first prepared by B.C. Brodie (13,p.249-259) in 1859 by the treatment of graphite with potassium chlorate and fuming nitric acid in a series of oxidation steps. Since then numerous investigators have suggested other methods of preparation or have improved on the original Brodie method. Some of these methods and improvements are summarized below.

Moissan (63,p.43-56) found that the time required for oxidation could be reduced by using anhydrous  $\text{HNO}_3$  and carefully dried  $\text{KClO}_3$ . Luzi (63,p.43-56) also shortened the process by subjecting the graphite to a preliminary oxidative and thermal treatment which reduced the graphite to a fine degree of subdivision.

Staudenmaier (68,p.1481-1487) claimed to have shortened the number of oxidation steps by using  $\text{KMnO}_4$  in the final steps instead of  $\text{KClO}_3$ . He also found that a mixture of concentrated  $\text{H}_2\text{SO}_4$  and  $\text{HNO}_3$  could be used to replace the fuming  $\text{HNO}_3$  used by Brodie. Charpy (21,p.920-923) showed that other oxidizing agents could be used, such as  $\text{H}_2\text{CrO}_4$  with  $\text{KMnO}_4$  and concentrated  $\text{H}_2\text{SO}_4$  with  $\text{KMnO}_4$ .

Modern investigators have found other methods for improving the oxidation process or have found new methods of preparing the oxide. Maire (56,p. 61-63) expedited the oxidation in the Brodie method by bubbling air through the reaction mixture kept for one hour in a 60°C water bath.

Graphite oxide was prepared electrochemically by Brown and Storey (15,p.129-147). A graphite anode was used in an acid or neutral electrolyte having an oxygen-containing oxidizing anion such as  $\text{HNO}_3$ . However, the product which collected in the bottom of the bath contained considerable unaltered graphite.

A rather unique method of preparing graphite oxide was claimed by Bottomely and Blackman (12,p.620). Benzene and other aromatic compounds were oxidized in a mixture of  $\text{H}_3\text{BO}_3$  and  $\text{H}_2\text{O}_2$  with  $\text{CuSO}_4$  as a catalyst. The temperature of the reaction mixture was kept at 90°C. A modification of the Staudenmaier method was devised by Hummers (49), in which graphite is mixed with  $\text{NaNO}_3$  and  $\text{H}_2\text{SO}_4$ .  $\text{KMnO}_4$  is then added with vigorous stirring. After heating and dilution the mixture is treated with  $\text{H}_2\text{O}_2$  and filtered.

### Physical Properties

Color. The most common color of graphite oxide appears to be yellow and brown. The oxide is usually green in the initial oxidation steps changing to the yellow or brown form in the final stages. Other colors such as blue and black have been reported, which also appear to occur in the initial oxidation steps. According to Thiele (72,p.145-160) these differently colored oxides have the same composition. He claims that the blue and the green forms change into the yellow and brown forms under the influence of red light rays.

In another article Thiele (74,p.1-20) reports that the different colors of graphite oxide are due to methods of purification, to physical structure, to particle size and to degree of purification. Water and various acids and alkalies appear to affect the color also.

Kohlschutter and Haenni (52,p.121-144) state that the color was dependent on the degree of dispersion of oxide particles. The color was independent of the graphite from which it was made. Clauss et al (22,p. 205-220) found that yellow graphite oxide darkens on exposure to light, on heating to 80°C, or on treatment

with sodium hydroxide or sodium ethoxide. This change may be reversed in an acid-oxidizing media. The color change was attributed to tautomeric equilibrium in which the keto form is darker than the enol. However, the composition appeared to remain constant.

Contrary to what has been said above, Hummers (50,p.1339) maintains that there is a definite relationship between color and composition. He claims that the lighter graphite oxides contain more oxygen than the darker ones.

Colloidal properties. Like graphite, graphite oxide is capable of only colloidal suspension. It is extremely hydrophilic; it swells in water and in many cases may even be peptized to a viscous gel (71, p.129-138). The "hydrosol" will form spontaneously not only with water, but also with ethanol, acetone and other liquids with high dielectric constants. On shaking with water the crystals separate into single layers which makes it a true eucolloid solution, since each layer is a molecule of molecular dimensions (41, p.351-357).

While the colloidal suspensions of graphite oxide are relatively non-conducting, the particles, themselves, are negatively charged in the entire pH range. They

will migrate to the anode on electrolyzing (71,p.129-138). On drying the oxide forms parchment-like sheets which can be peeled from each other like onion skins. The micellar solutions of graphite oxide may possess high viscosities which increase rapidly and non-linearly with concentration. The addition of flocculating agents such as salts of divalent metals produces gels that are essentially colloidal salts.

Hambdi (34,p.22-26) studied the coagulating power of different chlorides on the sol. He found the relative coagulating times were in the following order:  $\text{Li} > \text{Na} > \text{K} > \text{Rb} > \text{Cs} > \text{Mg} > \text{Ca} > \text{Sr} > \text{Ba}$ . Small amounts of alkaloids and other high molecular weight bases also coagulate the sols; however, the effect of corresponding acid substances is small (71,p.129-138). The graphite oxide sols are protected by humic and tannic acid and starch. Rapid coagulation produces amorphous particles, while slow coagulation gives rise to membranes.

#### Chemical Properties

Redox. The oxidizing power of graphite oxide has been known for some time. The oxide will liberate iodine from potassium iodide solutions; it will give a blue color to a solution of diphenylamine in

sulfuric acid, but will not decolorize indigo solutions. Carter et al (20,p.1305-1312) oxidized various aromatic amines by refluxing with graphite oxide. The reduction was fairly complete. From this study graphite oxide was deduced to have an oxidizing capacity similar to  $PbO_2$  and  $H_2O_2$ .

Thiele (72,p.145-160) has claimed that graphite oxide is quantitatively reduced to graphite by solutions of stannous and ferrous chlorides in HCl, in the presence of metals of the platinum group. However, Hofmann et al (45,p.1-41) observed that the oxide was not completely reduced. They found that aqueous  $FeCl_2$ ,  $N_2H_4 \cdot H_2O$  and  $H_2S$  caused the removal of 68, 82, and 92 per cent respectively of all the combined oxygen. The c-spacing of graphite oxide reduced by  $H_2S$  was shown by x-ray diffraction to be decreased to that of graphite (3,4).

Graphite oxide is also capable of electrolytic reduction. The graphite oxide particles migrate to the anode as mentioned above and slowly decomposes to form carbon dendrites upon reduction.

Acidity and ion exchange. According to Thiele (74,p.1-20) graphite oxide is a true acid because it will form salts in solutions of neutral salts or

alkalies. In water graphite oxide is in a chemically reversible equilibrium with its salts. The exchangeable hydrogen ions probably originate from the weak to strongly acid hydroxyl and carboxyl groups (64, p.381-417).

Hofmann and Holst (46, p.754-771) liberated acetic acid with graphite oxide in a sodium and calcium acetate solution. They found that the cation exchange capacity depended on the concentration of the salt solution and reached a maximum of approximately 1.8 meq./g. The exchange capacity of the oxide with LiOH and NaOH was 5.5 meq./g. at the maximum. The capacity with  $\text{Ba}(\text{OH})_2$  was higher; however, this value was discounted because of formation of  $\text{BaCO}_3$  resulting from decomposition of the oxide. Methylation with methyl alcohol and HCl gave a value of 3.6 meq./g. Treatment with diazomethane proves to be more effective in methylation because the product contained 4.5 meq./g.

Further study of methylation of partially decomposed specimens led to the belief that methylation with methyl alcohol and HCl acts preferentially on the peripheral acidic carboxylic and hydroxyl groups. From x-ray studies on methylated and unmethylated

specimens, Hofmann and Holst concluded that diazomethane methylates not only the peripheral groups but also the hydroxyl groups attached to the inner carbon atoms. Other investigators (63,p.43-56) have contested the results of these studies on the grounds that steric hindrance prevents complete methylation as it does in the methylation of humic acids.

Hamdi (35,p.554-634) titrated graphite oxide directly with NaOH. He got fleeting end points which he attributed to the presence of ethylene oxide groups capable of only hydrolyzing slowly. Indirect titration of the oxide suspended 16 days in varying concentrations of NaOH gave poorly defined breaks in the titration curve at 1.0, 2.75, and 5.25 meq. of NaOH. He associated these breaks with carboxyl, hydroxyl, and ethoxy groups. Back titrations with HCl to determine the amount of alkali retained in combination with graphite oxide showed that this combination increased in the order of  $\text{LiOH} < \text{NaOH} < \text{NH}_4\text{OH} < \text{KOH} < \text{Sr}(\text{OH})_2 < \text{Ca}(\text{OH})_2 < \text{Ba}(\text{OH})_2$ .

X-ray interference rings showed the presence of  $\text{BaCO}_3$  in graphite oxide treated with  $\text{Ba}(\text{OH})_2$ . On removal of the barium, these rings disappeared,

although no  $\text{CO}_2$  was evolved. This confirmed the findings of Hofmann and Holst given above.

Recently Claus et al (22,p.205-220) determined the exchange capacity of graphite oxide by titration with alcoholic KOH. They found the value 9.25 meq./g. which exceeded the value determined by titration with aqueous KOH (5.8-6.0 meq./g.) and methylation by diazomethane in dioxane (7.0-7.3 meq./g.).

Further investigations with alcoholic NaOH gave values approaching 9.0 meq./g. With a solution of sodium ethoxide in absolute alcohol the maximum value obtained was 10.5 meq./g. Treatment of graphite oxide methylated by diazomethane in dioxane with sodium ethoxide gave a total of 11.0 meq./g. This value approaches the number of meq. of hydrogen left in graphite oxide after extracting the molecular water with dioxane.

When methylated graphite oxide was treated with a NaOH solution, there was an ion exchange of 3.2 meq./g. and a saponification of 1.3 meq./g. of methoxyl groups. From this and other data Claus concluded that the weakest carboxyl groups are less acidic than the strongest hydroxyl groups and that the acidity of these hydroxyl groups was due to the proximity of double bonds (see Figure 1b).

Decomposition. Graphite oxide will deflagate when it is heated to approximately 200°C, leaving a light, fluffy residue similar to carbon black. At first it was thought that only CO and CO<sub>2</sub> were evolved (45,p.1-41); however, De Boer and Van Doorn (9,p.17-21) found that on rapid heating some molecular oxygen is expelled at first. This oxygen is later consumed in reactions to form CO and CO<sub>2</sub>.

The black residue from the decomposition is believed to be similar to graphite in its structure. It still contains some residual oxygen which may be removed by FeSO<sub>4</sub>, hydrazine or electrolytic reduction (43,p.613-618). It can also be removed slowly by heating, in which CO and CO<sub>2</sub> are evolved.

### Composition and Structure

Empirical formula. The composition and structure of graphite oxide has been a controversial subject since the substance was first prepared. It seems that one of the major problems has been to obtain the solid in a thoroughly dried state so that the true composition may be found. Drying has been done principally by evacuating the sample over P<sub>2</sub>O<sub>5</sub>, oven drying, leaching with ether and dioxane, freeze drying,

and heating under vacuum.

Examples of the empirical formulae found by early investigators are as follows:  $C_{11}H_6O_5$ ;  $C_{11}H_9O_6$ ;  $C_{24}H_9O_{13}$ ; and  $C_{14}H_4O_7$  (63,p.43-56). Balbiano (2,p.191-203) claimed that the composition varies with the method of preparation and the quality of graphite used. However, recent investigations have proved that this is not entirely true (8,p.12-16).

Thiele, one of the more modern investigators, proposed an empirical formula of  $C_6(OH)_3$  (72,p.145-160). However, Hofmann (42,p.112-114) and Ruess (65,p.17-26) (64,p.381-417) both disputed Thiele's formula. It was claimed that a well-washed and dried oxide had a lower hydrogen content. Ruess found no fixed stoichiometric relationship; for in his analyses, the C:O ratio varied between 6:1 and 6:2.5.

While other investigators found different C:H:O ratios, De Boer and Van Doorn (7,p.181-191), who prepared graphite oxide by the Staudenmaier method, obtained an empirical formula,  $C_7H_2O_4$ . They claimed that this ratio was independent of the type of graphite used in preparing the oxide.

Structure. Thiele (72,p.145-160) first postulated that graphite oxide had a cyclic structure with six

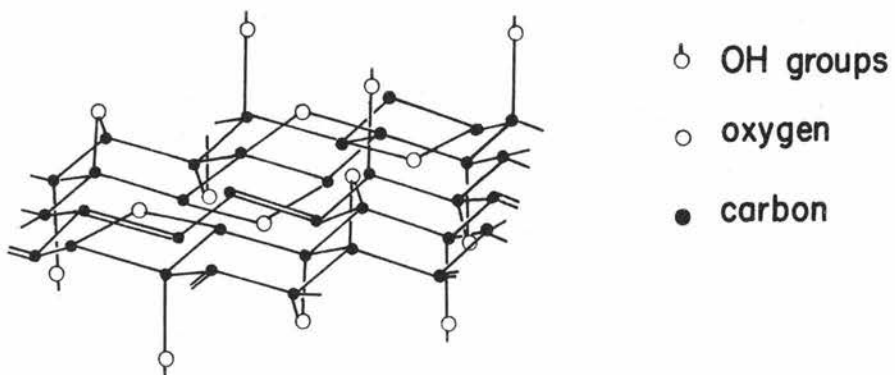
carbon atoms in the same configuration as the original graphite. Ruess (64,p.381-417) in his study of the crystal structure indicated that the carbon layers displayed an oxyaromatic character. X-ray investigations by Hofmann et al (45,p.1-41) established that the a and b axes in graphite oxide were more or less similar to graphite; however, the 001 or c-spacing was enlarged from 3.4 A to 6.3 A for the dried graphite oxide. Similar results were found by Derksen and Katz (25,p.652-669).

The hydrogen in graphite oxide is believed to be bonded to the carbon atoms as hydroxyl and carboxyl groups (40,p.435-441)(41,p.351-357)(74,p.1-20). While part of the hydrogen may be tenaciously retained as water, the hydroxyl and carboxyl groups can be distinguished by their chemical reactivity (22,p.205-220)(46,p.754-771). The carboxyl groups can be esterified, and at least part of the hydroxyl groups can be determined by estimating the amount of tightly bound hydrogen present after prolonged washing in dioxane and correcting for the number of carboxyl groups. Most preparations contained approximately one hydroxyl group for every six carbon atoms (64,p.381-417).

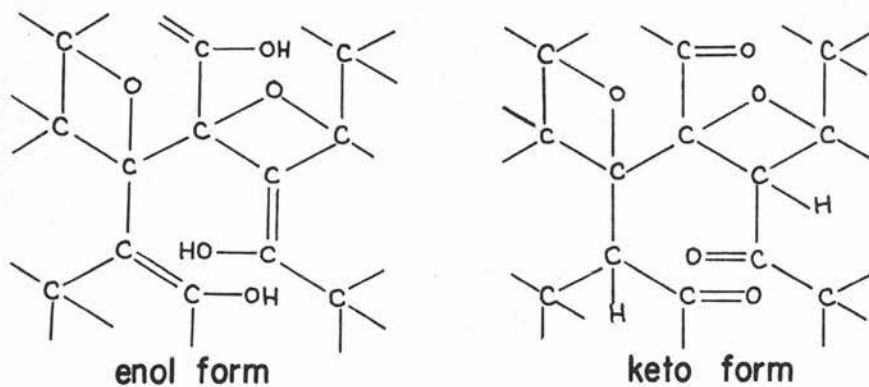
There is considerable doubt about the actual bonding of the oxygen to the carbon layers. It was originally believed that most of the oxygen in graphite oxide was bonded by ether linkages on adjacent carbon atoms (40,p.435-441). However, detailed chemical and structural analyses by Ruess (64,p.381-417) have supported the theory that ether linkages are probably in the meta positions. The carboxylic groups are present on the periphery of the graphite oxide crystallites. The influence of these carboxyl groups on the empirical composition increases when the particle size decreases.

An alternate suggestion was made by Carter et al (20,p.1305-1312) who proposed that the oxygen is present as peroxide groups connected to adjacent carbon layers. Another suggestion was made by Weiss (78,p.744-745) and more recently Franklin (30, p.50) who postulated a partly ionic type of structure. The positive charges are supposed to be in the form of single layers of carbon that have partially lost their pi bond character, and the anions are supposed to be in the form of multilayers of  $(O_x^-H_y)_n$ . These suggestions, however, do not appear compatible with the chemical properties of graphite oxide.

Figure 1  
Structure of Graphite Oxide



A. Structure of Graphite Oxide as suggested by Ruess



B. Structure of Graphite Oxide as suggested by Clauss et. al.

A structural model proposed by Ruess (64,p.381-417) is shown in Figure 1a. In this model the hydroxyl groups are a result of random disorder among the meta ether links, which will occasionally result in available bonds in para or even more remote positions than the required meta positions. Oxygen on such a position would presumably not form an ether bridge but rather a hydroxyl group. It should be noted that the model identifies the hydroxyl groups with tertiary alcohol groups. Any carboxylic groups would be at the periphery of the lattice plane. The warped structure in this model has been supported by other investigators (19,p.227-242).

Hofmann and coworkers criticized this model by pointing out that hydroxyl groups of graphite oxide are considerably more acidic than other tertiary alcohols. They submitted instead a structure in which the hydroxyl groups are vicinal to carbon double bonds. For such a model, the keto-enol tautomeric structure of Figure 1b can be drawn. This model predicts an ideal composition of  $C_8O_2(OH)_2$  for graphite oxide.

De Boer and Van Doorn (10,p.160-169) were also led to similar conclusions on the tautomeric forms of

graphite oxide by experimental evidence different from that of Hofmann. However, their criticism of Hofmann's model was its inability to show clearly why graphite oxide has oxidizing properties. They suggested that these properties are a consequence of a hydroperoxide character in the oxide. From their work they deduced the following possible combinations in addition to one keto-enol group for a  $C_7H_2O_4$  unit.

- (1) (-O-O-)(-OH)
- (2) (-O-O-H)(-O-)
- (3) (-O-)<sub>2</sub>(OH)

In order to help clarify the situation, Hadzi and Novak (31,p.1614-1620) undertook the infrared studies of graphite oxide. The absorption peaks indicated that the oxide contained carboxylic carbonyl, hydroxyl and possibly epoxy or peroxy groups. However, no bands were found which could be assigned to carbon double bonds.

Another important problem concerning graphite oxide is the planarity of the carbon layers. It would seem that the loss of the resonating double bond characteristics of graphite would result in a warped structure due to the tetrahedral configuration

of carbon sigma bonds. However, most experimental evidence is inconclusive. Perhaps the best piece of evidence is that of Beckett and Croft (3,p.929-935), who observed by use of electromicrographs, considerable folding of graphite oxide layers along no common plane. Such folding was not noted in the original graphite. This work would seem to support the warped structure of the model proposed by Ruess.

#### Adsorption of Vapors and Gases

As a result of oxidation, graphite oxide is strongly hydrophilic compared to the original graphite. Pallman (60,p.72-81) found that graphite oxide adsorbed 35.6 per cent of its weight in water as compared to graphite, 0.6 per cent, and acid lignin, 9.3 per cent, at a vapor pressure of 15.48 mm of Hg. He concluded from his studies that the hydrophilic nature was directly proportional to the degree of oxidation. This conclusion seemed reasonable on the basis of hydrogen bonding between the water molecules and the oxygen atoms in the compound.

Hofmann et al (45,p.1-41) obtained typical S-shaped curves in their determination of water vapor isotherms. The expansion of the basal (c) spacing was

measured as a function of the volume of water adsorbed, and the conclusion was made that the swelling of the graphite oxide was due to the physical adsorption of water between the platelets. However, it was considered that a 10 per cent water content remained at essentially zero pressure which could not be removed below 120°C.

Ruess (64,p.381-417) found a definite break in water vapor isotherms at nine mm. pressure. At this point 100 mg. of water per gram of sample was adsorbed. X-ray data indicated that the platelets had expanded from 6 to 9 Å. Ruess concluded that this expansion was due to the formation of a water monolayer between the carbon layers. The c-spacing was increased to 11 Å at the saturation point where 51% water was adsorbed.

In 1943 Hamdi (35,p.554-634) found from water vapor adsorption studies that, when he outgassed his samples, the isotherms exhibited hysteresis over the entire pressure range. Hamdi postulated that the first steep rise in his S-shaped isotherm was the result of chemical union of water with active groups. The middle portion of the curve was thought to result from the adsorption of water vapor on the exterior

surface of the particles resulting in very little intercrystalline swelling. At higher pressures the amount of adsorption increased more rapidly as the result of the carbon layers being pried apart.

De Boer and Van Doorn (11, p. 242-252) investigated the adsorption of  $N_2$  as well as water vapor adsorption on graphite oxide. They found that very little  $N_2$  was adsorbed in comparison with water vapor. The specific surface areas found by the B.E.T. method was 70-80  $m^2/g.$  from the  $N_2$  isotherms and 585  $m^2/g.$  from the water isotherms. Contrary to what was found by Hambdi, the water vapor isotherms obtained by these investigators for some samples had hysteresis loops which closed at approximately 0.4  $P/P_0$ ; however, other samples had hysteresis loops which also covered the whole pressure range. The  $N_2$  isotherms had hysteresis loops which closed at approximately 0.45  $P/P_0$ . The expansion of the c-spacing with water adsorption was investigated with x-rays. It was found that a water content of more than four per cent was necessary before any change in c-spacing was detected. Very little expansion was noted up to 16 per cent water; from this point the c-spacing increased linearly with increasing water content.

Slabaugh and Hatch (39,p.59) studied the adsorption of hexane as well as water vapor on graphite oxide. They obtained typical S-shaped isotherms with well defined hysteresis loops which covered essentially the entire pressure range. B.E.T. analyses indicated a surface area of approximately  $2.4 \text{ m}^2/\text{g}$ . from the hexane isotherms and approximately  $325 \text{ m}^2/\text{g}$ . from the water vapor isotherms. However, these areas are based on samples kept at 51 per cent relative humidity, while the areas found by De Boer and Van Doorn were based on dry weight.

The results of the studies from the last two groups of investigations will be discussed further in a different section.

#### Potential Uses of Graphite Oxide

To this date there are no practical uses for graphite oxide. However, there is great possibility that graphite oxide may be found useful because of its large oxidizing capacity. The present disadvantages in the use of graphite oxide are its difficulty and expense in production and its instability.

A possible use is given by Brown (14,p.113-118) who used it as a depolarizer to supplant or to sup-

plement the  $MnO_2$  in dry cells. Cells made with graphite oxide are similar to those containing  $MnO_2$ , except that they have a lower initial open circuit voltage. Graphite oxide made electrochemically is especially suited for this purpose because it contains a considerable quantity of graphite, which makes the oxide a better conductor of current.

According to Thiele (70,p.218) graphite oxide in gel form can serve as a nutrient medium for certain penicillium and Aspergillus species as well as spore forming bacteria. The graphite oxide is a source of carbon. Salts like  $(NH_4)_2SO_4$ ,  $K_2HPO_4$ ,  $MgSO_4$  and NaCl must be added to the gel to make it suitable.

Clauss and Hofmann (23,p.522) obtained membranes of graphite oxide, 0.03-0.05 mm thick, by the evaporation of a colloidal suspension of the oxide on a smooth glass surface. These membranes are permeable to water vapor but not to oxygen or nitrogen. The intracrystalline water layers equilibrate with the water vapor on both sides of the membrane while the oxygen and nitrogen cannot penetrate between the densely packed graphite layers. This method is not only applicable for the determination of vapor pressure of water but also that of other polar solvents, such as dioxane and alcohols.

## THEORETICAL BACKGROUND

Adsorption

Adsorption is a process in which the atoms or molecules of one material (adsorbate) become attached to the surface of another substance (adsorbent). The phenomena of adsorption was first mentioned by Scheele in 1773, who reported the results of experiments on charcoals exposed to gases.

There are two types of adsorption which are recognized at the present time. (1) Physical adsorption is essentially surface condensation due to the physical attraction of the surface of a material for a specific atom or molecule. It is sometimes referred to as van der Waals adsorption. (2) Chemical adsorption is due to the primary valence forces on the surface of a molecule. It is relatively strong and independent of the physical nature of the adsorbent. This adsorption may be considered as essentially chemical in nature and hence shows many chemical characteristics.

There are certain properties which are usually specific to the respective type of adsorption. In physical adsorption, the heats of reaction evolved are in the order of the heats of liquification.

Adsorption decreases rapidly and continuously with increasing temperature; it increases gradually with increasing pressure.

In chemical adsorption, the heats are usually in the order of that in a chemical reaction. (In some cases they are even endothermic). Adsorption increases and then falls with rising temperature. It increases rapidly with increasing pressure in the lower pressure regions, but it soon reaches a saturation value constant for a given temperature. If both chemical and physical adsorption occur simultaneously, sharp differentiation between them is impossible (79,p.31-39).

One of the first attempts to explain adsorption mathematically was made by Freundlich who used an empirical equation relating amount of gas adsorbed with pressure. The equation is as follows:

$$(1) \quad x/m = KP^{1/n}$$

where  $x/m$  is the weight of adsorbate per gram of adsorbent;  $P$  is the pressure, and  $K$  and  $n$  are constants. While this equation has been given theoretical significance (33,p.624-630), it contributes little to the over-all picture of adsorption.

Langmuir equation. Langmuir (53,p.1361-1403) produced one of the first and most important equations based on theory. He first postulated that gases adsorbed on a solid would not form a layer more than a single molecule in depth. Then he visualized that a dynamic equilibrium was formed in which the rate of condensation of molecules on the surface equaled the rate of their evaporation and that the actual rates were dependent on surface coverage. From these considerations he derived the following equation:

$$(2) \quad P/V = 1/V_m b + P/V_m$$

where  $V$  is the volume of gas (S.T.P.) adsorbed at pressure  $P$ ;  $V_m$  is the volume adsorbed when the surface is covered with a complete monolayer.  $b$  is a constant for any specific temperature.

The Langmuir theory is limited by the fact that it considers only a monolayer and that it predicts a saturation value for the amount of adsorption; however, it has been used successfully to explain some data on chemisorption. Adsorption systems that obey Langmuir's equation are considered ideal.

The B.E.T. equation. In 1937 Emmett and Brunauer (16,p.1553-1564)(17,p.2682-2689) and others pointed

to the fact that the long linear portion of many adsorption isotherms may represent the building of a second layer of adsorbed gas. Therefore, the beginning of this long linear portion ("point B") would represent the completion of a monolayer and could be used to determine surface areas of solids. However, the "point B" method failed to cover all adsorbates and adsorbents as some systems did not show any break (or very little) in the isotherms. Therefore, Emmett and Brunauer, with the help of Teller, developed the new classical B.E.T. equation (18,p.309-319) in order to calculate surface areas in systems not amenable to the "point B" method.

The B.E.T. theory is essentially an extension of Langmuir's interpretation of monomolecular adsorption into multilayer adsorption. The fundamental assumption was made that the same type of forces between molecules in vapor condensation also occurs in the phenomena of van der Waal's adsorption. It was further assumed that the heats of adsorption of all layers excepting the first were equal to the heat of liquification of the gas and that the ratio of the coefficients of adsorption and desorption in the multilayers were equal to each other. With these

assumptions the following equation was derived:

$$\frac{P}{V(P_0 - P)} = \frac{1}{V_m C} + \frac{c-1}{V_m C} \cdot \frac{P}{P_0}$$

This is a linear equation where a plot of  $P/V(P_0 - P)$  vs.  $P/P_0$  (saturation pressure) permits the slope and the intercept to be used for the evaluation of the constant  $C$  and  $V_m$ . The constant  $C$  is actually equal to  $a_1 b_2 / a_2 b_1 \cdot e^{E_1 - E_L / RT}$  where  $E_1 - E_L$  is the difference between the average heat of adsorption in the first layer and the heat of liquification of the adsorbate;  $a$  and  $b$  are coefficients of adsorption and desorption. This equation usually works quite well for  $P/P_0$  between 0.05 and 0.35.

With the knowledge of  $V_m$  one may calculate the surface area of a solid if the cross-sectional area of the adsorbate molecule is known. Emmett and Brunauer (17, p. 2682-2689) suggest using the following equation to find the area of the adsorbate molecule assuming close packing:

$$(4) \text{ Area} = 3.464(M/4 \cdot 2Nd)^{2/3}$$

in which  $M$  is the molecular weight;  $N$  is the Avagadro number, and  $d$  is the density of the liquified or

solidified gas. There is some controversy concerning the reliability of the adsorbate areas calculated from this equation. This in turn reflects on the reliability of the B.E.T. method of making surface area determinations.

One major criticism of the B.E.T. theory is that it does not provide for capillary condensations. Many refinements and new approaches have been made in order to eliminate the shortcomings of the B.E.T. equation. These, however, have usually resulted in long, unwieldy, expressions, none of which have any real advantage over the B.E.T. equation.

Harkins-Jura equation. Harkins and Jura (38, p.1366-1373) pointed out that for any condensed film on liquids or solids the film pressure ( $h$ ) is related to the area ( $s$ ) by the expression

$$(5) \quad h = b - as$$

where  $a$  and  $b$  are constants. This linear expression persists up to higher pressures where the film is several molecules thick. Because the film pressure is rather difficult to determine, an equivalent expression was derived:

$$(6) \quad \log P/P_0 = B - A/V^2$$

where A and B are constants, P is the gas pressure, and V is the volume of the adsorbed gas measured experimentally. This is a linear expression in which the slope equals A.

It was noted by Harkins and Jura that the surface area (s) of the adsorbent was proportional to the square root of the slope; that is:

$$(7) \quad S = K(A)^{1/2}$$

where K is a proportionality constant for a specific gas which can be found by independent means (37, p.1362-1366)(36,p.919-927).

A comparison of the areas determined by the B.E.T. method with those found by the Harkins-Jura method shows good agreement in most cases. The application and limitations of the two methods are discussed in detail by Harkins and Jura (36,p.1366-1373) and by Emmett (28,p.1784-1789). Attempts have been made to rationalize the agreement between these two methods, but a complete and satisfactory method has not yet been given.

### Heats of Adsorption

All adsorption processes are accompanied by a

decrease in free energy because there are present at the surface certain unbalanced or unsymmetrical forces which are satisfied to a certain extent by the adsorption or desorption of an adsorbate. The free surface energy ( $\Delta F$ ) is decreased and the entropy ( $\Delta S$ ) is likewise decreased. Since

$$(8) \Delta H = \Delta F + T\Delta S$$

physical adsorption processes are always exothermic, and chemical adsorption is also exothermic except in rare cases.

Heats of adsorption are usually determined by two different methods. The first method is direct calorimetric measurement. A volume of gas is admitted to the surface of the solid, and the heat evolved is calculated from the rise in temperature. This is the average heat evolved for a specific part of the surface covered and is also known as the integral heat of adsorption. A modification of the differential heat of adsorption is the heat evolved when an infinitesimal amount of gas is adsorbed. This differential heat can be determined approximately in the calorimetric method by adding minute quantities of gas at a time to the surface.

The second method of measuring heats of adsorption is known as the isosteric method. To find the isosteric heat it is necessary to determine the equilibrium pressure corresponding to a given weight of gas adsorbed at various temperatures. The heat ( $\Delta H$ ) is then calculated by the use of the Clausius-Clayron equation:

$$(9) \quad dP/P = \Delta H_1/RT^2 dT/T$$

or upon integration

$$(10) \quad \log P = -\Delta H_1/2.3R \cdot 1/T + C$$

H is found from the slope,  $-\Delta H/2.3R$ , of the line which results from plotting  $\log P$  versus  $1/T$ .  $\Delta H$  may also be determined from this equation when it is integrated between limits.

$$(11) \quad \log P_1/P_2 = \Delta H_1/2.3R (1/T_2 - 1/T_1)$$

If no external work is done during the adsorption, the true differential heat,  $\Delta H_d$ , is obtained. It is possible to show by the use of thermodynamics that

$$(12) \quad \Delta H_1 = \Delta H_d + RT$$

It is likely that in practice the "calorimetric

differential heat" is intermediate between the true differential heat and the isosteric heat depending on how much PV work is transferred to the calorimeter as heat. However, the difference,  $RT$ , is normally lower than the error of measurements. (76,p.145).

The differential heats of chemisorption normally decrease markedly as the amount of adsorption increases. This decrease has been attributed by some workers to surface heterogeneity in which sites of lessening activity are covered as adsorption proceeds. It has, however, been suggested that the surface is uniform and that the effect is due to increasing surface repulsions between neighboring atoms (76,p.12).

There has been some disagreement among investigators concerning the validity of isosteric heats on systems which are not strictly reversible (have hysteresis effects). However, other investigators have found good agreement between the isosteric heats and the calorimetric heats even though the systems were irreversible. Emmett and Joyner (51,p. 2353-2359) measured the isosteric heats of adsorption of nitrogen on carbon black and found excellent agreement, with the calorimetric heats determined by Beebe et al (4,p.95-101). Foss and Reyerson

(29,p.1214-1216) calculated heats of adsorption on lyophilized ribonuclease which agreed quite well with those measured calorimetrically by Amberg (1,p.3980-3984).

### Infrared Absorption

Infrared spectra of adsorbed ammonia. A large variety of problems related to the nature of both physical and chemical adsorption processes have been studied by infrared spectroscopy. One of the problems in studies of this type is the correct interpretation of results since there are no exact counterparts in ordinary compounds with which to make comparisons. However, most interpretations are still made by comparing with conventional compounds. Good results have been obtained in this manner which are consistent with those obtained from other experimental procedures. Problems in chemisorption on metal catalysts seem to be most applicable to infrared studies (27,p.194-201).

Most of the studies made on physical adsorption systems have involved surfaces which have OH groups. Siderov (66,p.1235-1238) studied the effect of gases physically adsorbed on porous glass. He found that  $\text{NH}_3$  caused the OH band at  $7,300 \text{ cm}^{-1}$  to shift  $120 \text{ cm}^{-1}$ . He also observed bands at  $3,430$  and  $3,400 \text{ cm}^{-1}$ . Yates

(80,p.1980-1981) and his coworkers also studied the effect of  $\text{NH}_3$  on porous glass. They found a new band at  $2,900 \text{ cm}^{-1}$ , which they attributed to OH vibration in the hydrogen bonded group  $\text{O-H}\cdots\text{N}$ .

Mapes and Eischens (57,p.1059-1062) used infrared spectroscopy to study the chemisorption of ammonia on a silica-alumina cracking catalyst. They found bands at  $3,330 \text{ cm}^{-1}$  (N-H stretching vibration) and at  $1,640 \text{ cm}^{-1}$  (unsymmetrical bending vibrations) which were attributed to ammonia chemisorbed as  $\text{NH}_3$ , and small bands at  $3,130 \text{ cm}^{-1}$  and  $1,450 \text{ cm}^{-1}$ , which were attributed to  $\text{NH}_4^+$  ion. The  $1,450 \text{ cm}^{-1}$  band increased in intensity when the samples were exposed to moisture, while the  $3,330 \text{ cm}^{-1}$  decreased in intensity. The increase of  $\text{NH}_4^+$  and the decrease of  $\text{NH}_3$  was believed to be due to the reaction of  $\text{NH}_3$  with protons formed during the adsorption of water.

Similar bands were found in the same region for a variety of amines in which  $\text{NH}_3$  is coordinated with metals, such as Cu, Pt, Ni, and Cr. (69,p.6159-6163). These results indicate that the nitrogen bond with the catalyst does not alter the position of the bands. Analogous results are also obtained when  $\text{H}_2\text{S}$  and  $\text{H}_2\text{O}$  are chemisorbed on Pt and  $\text{SiO}_2$ ,

respectively. The S-H and O-H stretching bands appear at a position close to those found for  $\text{H}_2\text{S}$  and  $\text{H}_2\text{O}$  in a gaseous state. The conclusion may be drawn that coordination bonds between a surface and a central atom has little influence on the single bond vibrations of hydrogen--particularly the stretching vibrations.

Although the N-H stretching and the unsymmetrical bending vibrations are not markedly affected by coordination bonding of nitrogen to other atoms, the symmetrical N-H bonding vibrations, which appear as a doublet near  $955\text{ cm}^{-1}$  in gaseous  $\text{NH}_3$ , are shifted to shorter wave lengths in coordination compounds. However, this band, which should appear at approximately  $1335\text{ cm}^{-1}$ , is generally not found when  $\text{NH}_3$  is chemisorbed on a solid.

Infrared spectra at low temperatures. It has been found (48,p.1063-1076) in infrared studies on certain solids at low temperature that both the lattice and the molecules may be regarded as being in a very low energy state. The infrared spectra obtained under these circumstances are as simple as they can be for the solid since all the anharmonic effects are minimized, and one has essentially pure vibrational transition. Therefore, the infrared bands ob-

tained at very low temperatures should be exceedingly sharp and intensified. This was found to be true in some regions by Hornig and Wagner in studies on ammonium salts (77,p.296-304). They found that the intensity approximately doubles in the bands at 3,080, 3,140, and 1,760  $\text{cm}^{-1}$  from 29°C to -190°C and that very high resolution was obtained.

### X-ray Diffraction

Since the development of the Bragg theory in 1912, x-rays have been used to study the internal structure of a crystal. If the wave length of the x-ray is known, it is possible to measure the distance between planes in a crystal. This method is, therefore, directly applicable for use in measuring the (001) or c-spacing in laminar compounds such as montmorillonite clays, graphite, and graphite oxide.

Hofmann (44,p.1248-1262) was one of the first to use x-rays to study the basal spacing for graphite oxide. He found that the c-spacing had been expanded from 3.4 Å for the original graphite to 6.1 Å. This spacing could be increased to 11 Å by reversible swelling with water. Since then, extensive studies have been made on graphite oxide.

Some of the most important work has been done by MacEwan et al (55,p.677-682) who studied the swelling of graphite oxide as well as montmorillonite clays in contact with polar organic compounds. The basal spacing of the oxide was reversibly expanded up to as high as 48 Å with certain diamines.

#### EXPERIMENTAL PROCEDURES

##### Sample Preparation

The samples used in this work were prepared by two different methods from Canadian graphite No. 5 obtained from the Asbury Mills, Asbury, New Jersey. The material was 99 per cent pure, and its particle size was less than  $35\mu$  in diameter. The graphite was given no previous treatment before oxidation.

The Conventional Brodie Method. The samples, 2a, 2b, 2c, and 2d were prepared by the conventional Brodie method (13,p.249-259). Twelve and a half ml. of  $\text{HNO}_3$  were added to each gram of graphite, and the subsequent mixture was placed in an ice bath. Five grams of  $\text{KClO}_3$  were then added at a rate designed to keep the reaction from becoming too violent. After the addition of  $\text{KClO}_3$  was completed, the mixture was

placed in a water bath and kept at approximately  $50^{\circ}$  for 20 hours, after which the contents were poured into 20 milliliters of distilled water. The sample was washed three times with distilled water; after each washing the mixture was centrifuged, and the liquid was decanted from the residue. After the final washing, the residue was left in an oven overnight to dry at  $80^{\circ}\text{C}$ . This procedure was repeated for a total of five oxidation steps.

The Modified Brodie Method. The samples 1-P57a, 1-P58a, and 1-P91a were prepared by the modified Brodie method (56, p.61-63). Red fuming  $\text{HNO}_3$  was mixed with graphite, and this mixture was also placed in an ice bath. The  $\text{KClO}_3$  was added to the contents at such a rate as to keep the reaction mixture between  $35-45^{\circ}\text{C}$ . The flask was then placed in a  $55^{\circ}\text{C}$  water bath for an hour. During this time  $\text{N}_2$  was bubbled through the mixture at a rate sufficient to keep the mixture well agitated. The  $\text{N}_2$  and residual gases from the reaction were allowed to escape into a hood. After this, the mixture was poured into an equal volume of water, and the sample was washed as in the regular Brodie method. After drying for approximately 24 hours at  $70-80^{\circ}$ , the dried cake was

crushed, and the process was repeated for a total of five oxidation steps. The proportions of  $\text{HNO}_3$  and  $\text{KClO}_3$  to a gram of graphite are given here for each step:

- Step 1. 15 ml.  $\text{HNO}_3$ , 10 g.  $\text{KClO}_3$
2. 15 ml.  $\text{HNO}_3$ , 8.4 g.  $\text{KClO}_3$
3. 13 ml.  $\text{HNO}_3$ , 7.5 g.  $\text{KClO}_3$
4. & 5. Same proportions as step 3.

When large quantities of the oxides were prepared, care had to be taken to add  $\text{KClO}_3$  at a rate which kept the temperature at approximately  $40^\circ\text{C}$ . If the chlorate was added too slowly, the reaction slowed down or stopped until heat was applied. This created a dangerous situation when the mixture was placed in the water bath. For if the reaction was not sufficiently complete, it would react rapidly and beyond control when in the water bath. By the same token, if the chlorate was added too rapidly, the reaction mixture would heat up, and the reaction would soon be beyond control. Also, if the reaction mixture was in a constricted container, it was necessary to keep the gases (mostly  $\text{ClO}_2$ ) from accumulating too rapidly, as this would lead to a dangerous explosion. Because

of this situation, it was necessary to have the  $N_2$  bubbling rapidly through the delivery tube before placing it in the reaction mixture to prevent an accumulation of gases in the tube.

Sample processing. After the final oxidation step in both processes, the graphite oxide was purified by electro-dialyzing it for approximately 48 hours in a Mattson cell using untreated cellophane as the membrane. The applied voltage was brought up slowly to 350 volts. The electrode polarity was reversed periodically to prevent excessive accumulation of material on the membrane at the anode side of the cell. Copper was used for the cathode, while platinum was used for the anode.

After the current across the electro-dialysis cell reached a constant value, the product was removed and freeze dried. The wet slurry was swirled in a round-bottom flask cooled with a dry-ice - acetone bath until the mixture was frozen. The flask was then placed in an ice-water-salt bath to keep the mixture frozen while a vacuum was kept on the system. The vapor sublimed from the frozen product and was condensed in a dry ice - acetone trap which had to be emptied several times a day. The graphite oxide

dried in this manner was quite fluffy and easy to handle in comparison to that which was air or oven dried.

Samples 1-P57a and 1-P58a were prepared in the same batch; however, the batch was split in half. The first half (1-P57a) became partially thawed during the freeze drying process and was re-frozen. This seemed to change some of its characteristics; it seemed more dense than 1-P58a. Other changes will be seen later in another section.

In the first experiments (with samples 2a,2b,2c, and 2d) the basis of weight was graphite oxide vacuum dried at less than 0.1 mm pressure for 24 hours. However, this basis was subject to error even though the weight remained constant after a given period. Therefore, the graphite oxide was stored in a desiccator over a saturated  $\text{Ca}(\text{NO}_3)_2$  solution which maintains a relative humidity of 51 per cent. The moisture content of graphite oxide kept in this manner was between 17-19 per cent as shown in Table 1A. This percentage was in turn based on samples dried for three hours at  $160^\circ\text{C}$ . The graphite oxide dried at  $160^\circ$  had an apparent moisture content approximately one per cent higher than that which was vacuum dried.

TABLE I

## A. Composition of Graphite Oxide

<u>Sample No.</u>	<u>%C</u>	<u>%O</u>	<u>%H</u>	<u>%ash</u>	<u>%H<sub>2</sub>O @51% R.H.</u>	<u>C:O ratio</u>
<u>Conventional Brodie Method (vacuum dried)</u>						
2a	50.05	46.92	3.03	<0.1	---	1.43:1
2b	50.71	46.19	3.09	<0.1	---	1.46:1
2c	51.71	45.70	3.13	<0.1	---	1.51:1
2d	51.15	45.97	2.87	<0.1	---	1.48:1
<u>Modified Brodie Method (vacuum dried)</u>						
1-P57a	55.53	42.24	2.23	<0.01	---	1.75:1
1-P58a	55.48	42.00	2.52	<0.01	---	1.76:1
<u>Samples Oven Dried @160° for 3 hours.</u>						
2d	51.61	45.27	3.10	---	12.95	1.52:1
1-P57a	---	---	---	---	18.05	---
1-P58a	55.27	41.76	2.97	---	19.31	1.77:1
1-191a	55.32	42.14	2.54	---	17.74	1.75:1

## B. Concentration of Metal in Graphite Oxide Salts

<u>Metal</u>	<u>Li</u>	<u>Na</u>	<u>K</u>	<u>Rb</u>
<u>Concentration meq./g.</u>	2.00	1.61	1.09	0.83

This appears logical because undoubtedly some decomposition takes place at this temperature giving a higher loss of weight upon drying.

The temperature,  $160^{\circ}\text{C}$  was chosen as the standard drying temperature for a number of reasons. First, it was found by differential thermal analysis (39, p.84) that graphite oxide appears to lose all of its water between  $115-130^{\circ}\text{C}$ , while complete decomposition did not take place until above  $200^{\circ}\text{C}$ . Second, it has been found by x-ray diffraction (19, p.227-242) that on drying, the basal spacing reaches a minimum at approximately  $140-150^{\circ}\text{C}$ . Matuyama (58, p.215-219) in his pyrolysis studies of graphite oxide found a definite break in the loss of weight when the graphite was heated to  $150-160^{\circ}\text{C}$ .

There appears to be little difference between the structure and composition of vacuum dried and oven dried (at  $160^{\circ}\text{C}$ ) graphite oxide. This was demonstrated by infrared analyses and by carbon-hydrogen determinations (Figure 1A). The analyses for carbon and hydrogen were made by Drs. Weiler and Strauss, 164 Banbury Road, Oxford, England.

Graphite oxide salts. The graphite oxide salts were prepared by ion exchange with graphite oxide

prepared by the modified Brodie method. After electro-dialyzation, the graphite oxide was divided into four aliquots. Each aliquot was then mixed with a 10 per cent salt solution and stirred for two hours. This ion exchange was carried out batch-wise five times. Each time the mixture was centrifuged, washed, and the liquid decanted from the sample. After the final washing the samples were dialyzed to eliminate free salt, and then freeze dried.

The salts used were the chlorides of Li, Na, K, and RbI. An analysis was made on the final product to determine the amount of exchange by leaching twice with 6 N  $H_2SO_4$ . The eluents were dried, and the residual salt ( $Na_2SO_4$ ) was burned at  $800^\circ C$  to eliminate any adsorbed carbonaceous material. The results of these analyses are shown in Table 1B in meq. of metal ion exchanged per gram of vacuum dried sample. The graphite oxide salts seemed to decompose at  $160^\circ C$ ; therefore, the samples vacuum dried at less than 0.1 mm pressure were used as a basis for any work done on them.

#### Absorption Apparatus and Procedure

Description of apparatus. The absorption of

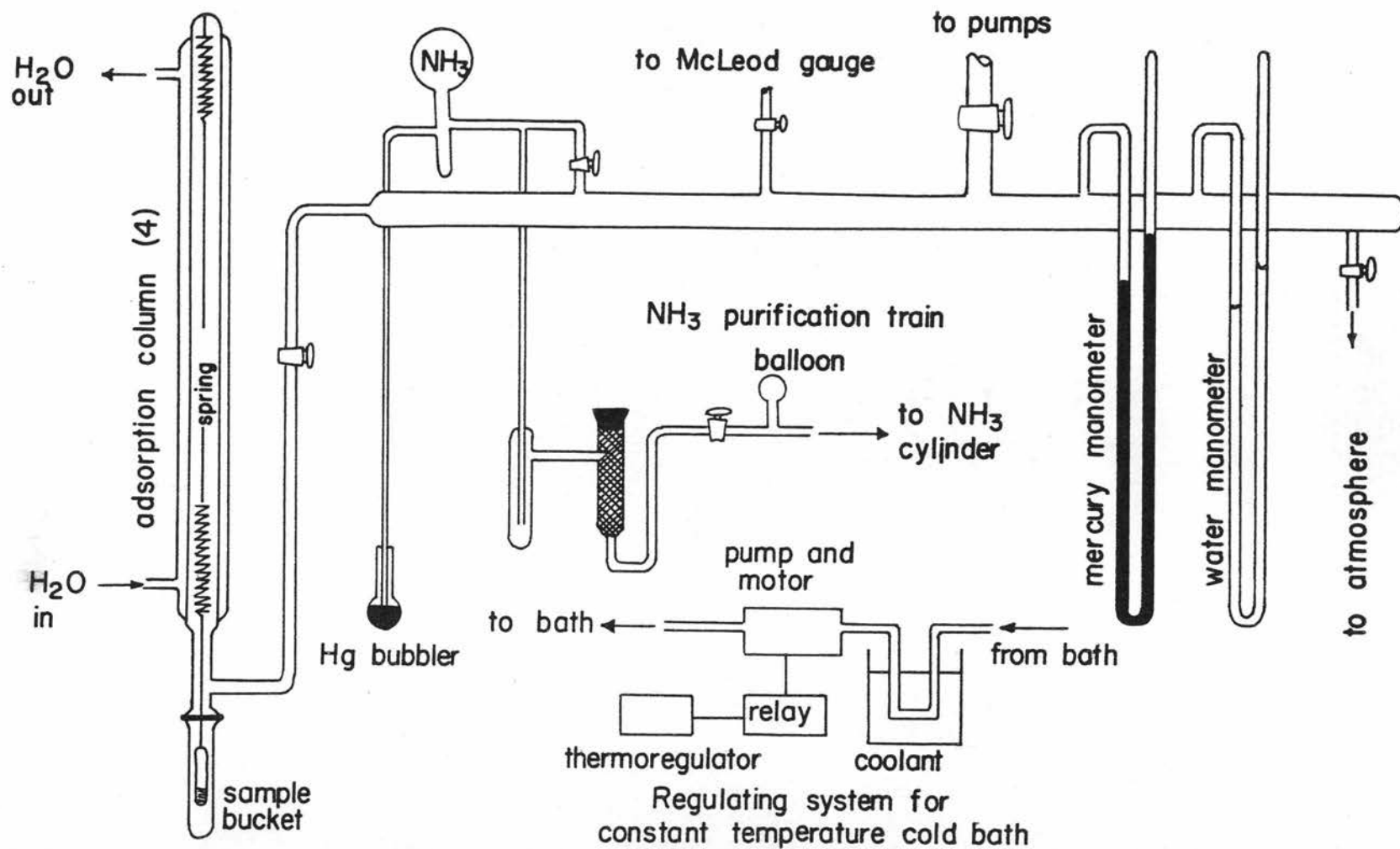
ammonia on graphite was measured gravimetrically instead of volumetrically because of the greater simplicity and accuracy of this type of measurement.

A schematic drawing of the absorption apparatus is shown in Figure 2. It consists essentially of a long absorption column with a water jacket with which the column can be thermostated at a constant temperature (28°C). At the bottom of the column is a ball joint to which a sealed glass tube may be attached with Apiezon W wax in order to enclose the sample. There were four of these columns connected to the rest of the absorption system.

A copper-beryllium spring was suspended from the top of each column. These springs were copper-beryllium alloy 25 ASTM B 194 obtained from the Beryllium-Copper Supply Company. A small glass fiber marked at approximately two cm intervals was hooked to the bottom at the spring. A second glass fiber supporting the sample bucket was hooked to the lower end of the marked fiber. The sample containers were tin foil buckets which weighed approximately 0.2 g.

The change in weight of the sample on absorption was determined by measuring the extension of the spring. This was done with a cathetometer sighted on one of

Figure 2  
Gravimetric Adsorption Apparatus



the markings on the above-mentioned glass fiber. The amount of deflection was read on a vernier scale on the side of the cathetometer. This scale could be read to  $\pm 0.1$  mm, or approximately  $\pm 0.2$  mg. since the sensitivities of the springs were around 2.0 mg./mm.

The system was evacuated through a dry ice - acetone cold trap by a Welch Duoseal forepump and a two stage mercury diffusion pump. Pressures lower than  $0.1\mu$  could easily be attained. The pressures in this region were measured with a McLeod gauge. Pressures in the range below 2 cm. were measured with an oil manometer (Apiezon B) which is about 15.5 times as sensitive as the mercury manometer used for pressures above 2 cm.

The samples were submerged in a constant temperature bath during an experiment. Isopropyl alcohol was used mainly to fill the reservoir as coolant. This alcohol had to be redistilled after each experiment because of contamination with condensed water vapor, which caused freezing and blocking of the lines. The liquid was cooled by pumping it with a gear pump and later by a Sigmamotor through a copper coil submerged in a dry ice - isopropyl alcohol bath. The pump was controlled by a Cenco bimetallic thermoregulator

through an electronic relay. The bath was kept well agitated with an electric stirring motor. The temperature was measured with an alcohol thermometer capable of being read to  $\pm 0.2^{\circ}\text{C}$ .

The ammonia gas was purified before use by allowing it to flow through a tube containing CaO into a dry ice - acetone trap where it was liquified. The system was then evacuated with an aspirator to expell any volatile gases. The liquified  $\text{NH}_3$  was warmed slightly in order to form gas to help sweep the system. The ammonia was then slowly distilled into another dry ice - acetone bath where it was again liquified. The ammonia was stored in the liquid state until it was ready for use. A balloon was attached to the purification train to prevent the gas pressure from becoming at any time greater than atmospheric pressure and blowing out the stopcocks.

Procedure. Samples of graphite oxide that had been stored at 51% relative humidity were weighed in tin foil buckets. Approximately 0.4 - 0.6 g. of sample was used, or approximately 0.8 g. total weight. In most cases the gain or loss of weight from the atmosphere was negligible in the time it took to weigh a sample; therefore, no precautions were necessary. The buckets

were then suspended from the tiny glass rods which in turn were attached to the marked rods hanging from the springs. These extra glass rods were used in order to bring the buckets to a desired level. The tubes were then sealed and the evacuation of air began.

The pressure was lowered slowly to less than 0.1 mm Hg in 24 hours. Then the pressure was lowered to 0.1  $\mu$  or less, and outgassing was continued for two more days. The samples were submerged in a constant temperature bath, and the zero point reading was taken with the cathetometer.

When the isobars were determined, the coolant used was water down to 0° where it was then changed to isopropyl alcohol. The ammonia was added to the system until arbitrary pressure was attained. After equilibrium was reached, a spring deflection reading was taken, and the temperature was lowered approximately 10°. More gas was added to the system to keep the pressure constant. A reading was again taken when equilibrium was reached, and the procedure was continued until the temperature was down to -45°. This same procedure was followed for various pressures. The pressure was regulated manually and could be kept constant with an oil manometer to  $\pm$  0.05 mm. Equili-

brium was reached in three to ten hours depending on sample, temperature, and pressure.

With the isotherms, only a constant temperature bath of isopropyl alcohol was used. An appropriate increment of  $\text{NH}_3$  was added; after equilibrium was reached, both a pressure reading and a spring deflection reading were taken. Ammonia was again added, and the same procedure was followed as before until the end of the run.

### Infrared Absorption

Attempts were made to obtain the infrared absorption spectra of graphite oxide from thin films of the compound on KBr plates. A fine suspension of graphite oxide in either ether or acetone was sprayed on the heated KBr plates with an atomizer. The ether or acetone evaporated on contact with the salt and left a thin film of the oxide. Unfortunately, the scatter of infrared radiation, especially in the region of lower wave length, was too great to obtain good spectra from these film.

Nujol and perflurokerosine mulls also gave poor results as far as scattering was concerned. The nujol mulls of graphite oxide had the added dis-

advantage in that the nujol peaks overlapped a major peak for graphite oxide.

Much better results were obtained from graphite oxide pressed with analytical grade potassium bromide into small disks (pellets). The KBr was ground reasonably fine with a mortar and pestle and then dried overnight at  $110 - 120^{\circ}$ . Approximately 1.2 mg. of graphite oxide were then mixed with 200 mg. of the dried salt, and the mixture was ground extremely fine in a vibrating micro-ball mill. The material was then placed in a pellet die and pressed under a pressure of 20,000 psi for several minutes in a hydraulic press. The pressure was released, and the pellet was removed from the die. The pellet was mounted on a cork with a hole bored through the center, and the spectrum was taken of the sample.

The infrared spectrophotometer was a Perkin-Elmer model 21 double beam instrument. Both LiF and NaCl prisms were used from the  $4000-2000 \text{ cm}^{-1}$ . The difference in the spectra from these two prisms was negligible in this region. Only the NaCl prism was used in the  $2000-650 \text{ cm}^{-1}$  region.

The spectra were taken on samples that were oven dried at  $160^{\circ}$  for three hours and samples that were

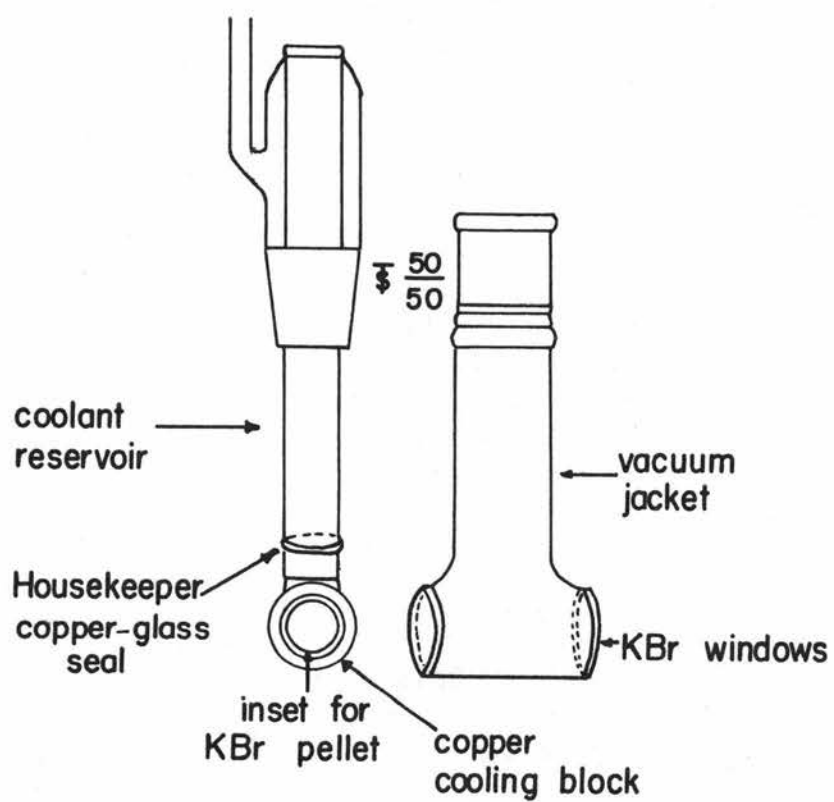
outgassed for two days at less than 0.1 pressure. Spectra were also taken of graphite oxide left in an atmosphere at 51% relative humidity. The samples with adsorbed  $\text{NH}_3$  were obtained either from the adsorption runs above or were prepared specially with only about one monolayer of gas absorbed on the sample.

A sample of graphite oxide vacuum dried for two days and a sample with a monolayer of  $\text{NH}_3$  adsorbed on it were sent to Dr. E.R. Lippincott (54,p.137-143) who made an infrared absorption spectrum on each sample with a special apparatus which he developed. The samples were pressed between two diamond crystals with enough pressure to make the sample transparent to infrared radiation. The spectra were taken in an inert atmosphere with a double beam Beckman spectrophotometer, model IR4, with a NaCl prism.

The spectra were also taken of samples cooled to liquid air temperatures in order to obtain better resolution from the peaks. The sample (in KBr pellets) was mounted in a specially constructed cell (Figure 3). The cell was assembled and connected to the vacuum system, and a hard vacuum (0.1 ) was pulled in the vacuum jacket. Then liquid air was poured slowly into the reservoir until the sample was cooled and

Figure 3

Infra-red absorption cell for  
use at low temperatures



an excess of liquid air remained in the reservoir. After the sample was cooled, the cell was placed in the infrared beam. The vacuum around the reservoir and sample holder prevented moisture from condensing on the KBr windows.

### X-ray Diffraction

X-ray diffraction studies were made on samples 1-P57a and 1-P58a with various quantities of ammonia adsorbed on them. The adsorption was done at room temperature because it was nearly impossible with the equipment available to maintain a constant temperature while taking x-rays of the samples. This provided a source of error because of fluctuations of room temperature; however, the error should not be over one to two per cent.

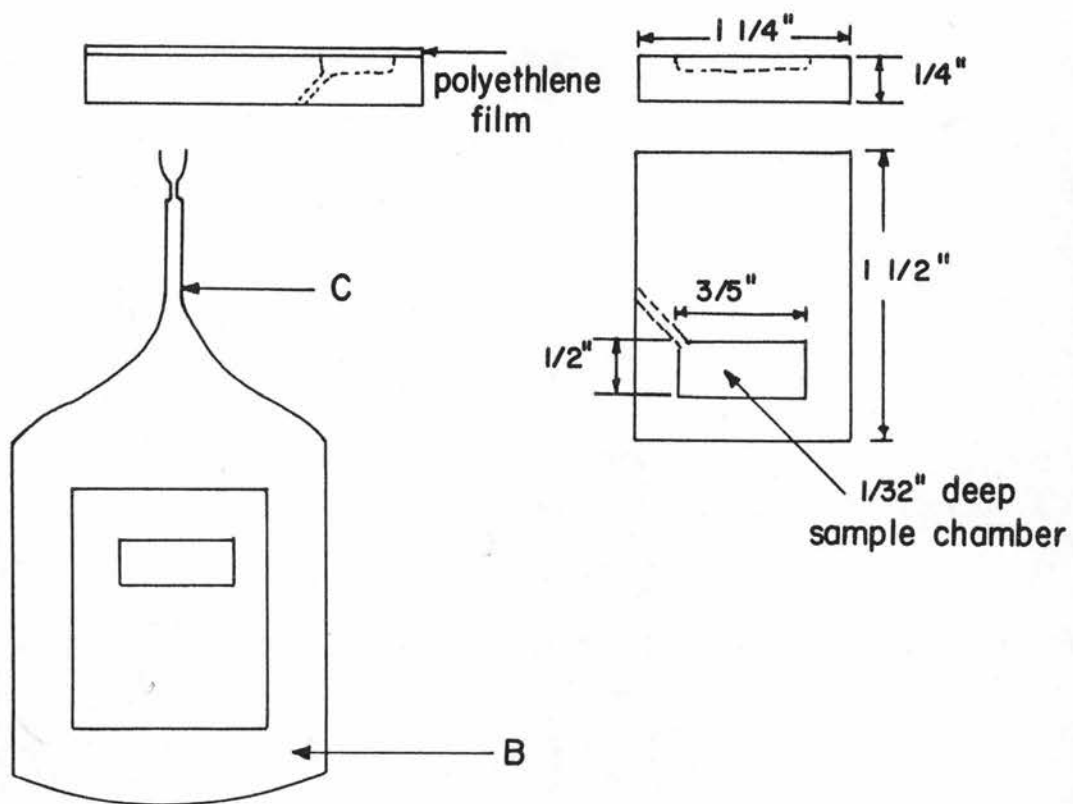
An x-ray spectrograph was used at first; however, the bands were too diffuse and could not be measured accurately. Also, the method was too time consuming to be practical. Therefore, a Norelco-Philips x-ray diffractometer with the  $K_{\alpha}$  band from a copper target was used. The wavelength was 1.54050 Å.

In the initial experiments samples of graphite oxide were placed in glass tubes which were then sealed

to the vacuum system used for the adsorption work previously mentioned (Figure 2). The adsorption on a weighed sample was measured under the same conditions in order to determine the weight of  $\text{NH}_3$  adsorbed per gram of sample. When a given amount of  $\text{NH}_3$  was adsorbed on this control sample, one of the tubes was sealed off from the vacuum system. This tube was broken, and the graphite oxide was placed in a standard sample holder. The x-ray diffraction was made immediately on the sample. Since the sample was exposed to the atmosphere, it either lost  $\text{NH}_3$  or adsorbed moisture from the air giving erroneous results. However, the initial work done on 1-P57a did show that a sample exposed to the atmosphere gave a limited c-spacing of 7.37 A, no matter how much  $\text{NH}_3$  was originally adsorbed on the sample.

To combat the above mentioned source of error, a new type of sample holder was designed and built from plexiglass. This sample holder is shown in Figure 4. The dimensions given are only approximate since they are not critical. The graphite oxide previously dried to insure proper packing was placed in the sample chamber (A) and packed tightly with a spatula. Then a piece of 0.012 mm polyethylene sheeting

Figure 4  
Sample Holder for X-ray Diffraction Studies



was glued with rubberized cement to the top of the sample holder, sealing in the sample. The edges were trimmed and sealed with glyptal paint to prevent leakage through any channels in the cement. A minute hole drilled through the plastic from the side of the holder provided access of the  $\text{NH}_3$  to the sample.

The holder containing the sample was sealed in a large glass tube (B) which was connected to the vacuum system by the smaller tube (C). After the desired quantity of  $\text{NH}_3$  was adsorbed on the sample, this tube was sealed off, with a torch, from the rest of the system. Immediately before the diffraction was made, the tube (B) was broken in a dry box under an inert atmosphere of  $\text{N}_2$  or A, and the small hole was sealed with a silicone grease. Caution had to be exercised in breaking the tube to prevent glass particles from piercing the polyethylene covering. In the last experiment a deposit of silicone grease was sealed in the tube (B) with the sample holder, and before the tube was broken, the sample holder was moved back and forth over this grease until the pin hole was sealed. The results from this method appeared to be the same as that of the first one.

The polyethylene cover did not change the value

of the c-spacing; however, it did diminish the x-ray intensity considerably. A possible source of error in this procedure was the fact that the polyethylene sometimes contained minute holes which, unless it was inspected carefully with a magnifying glass, sometimes escaped detection.

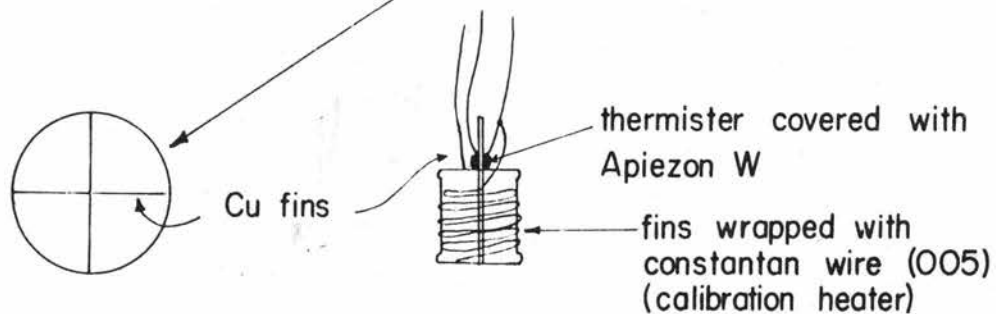
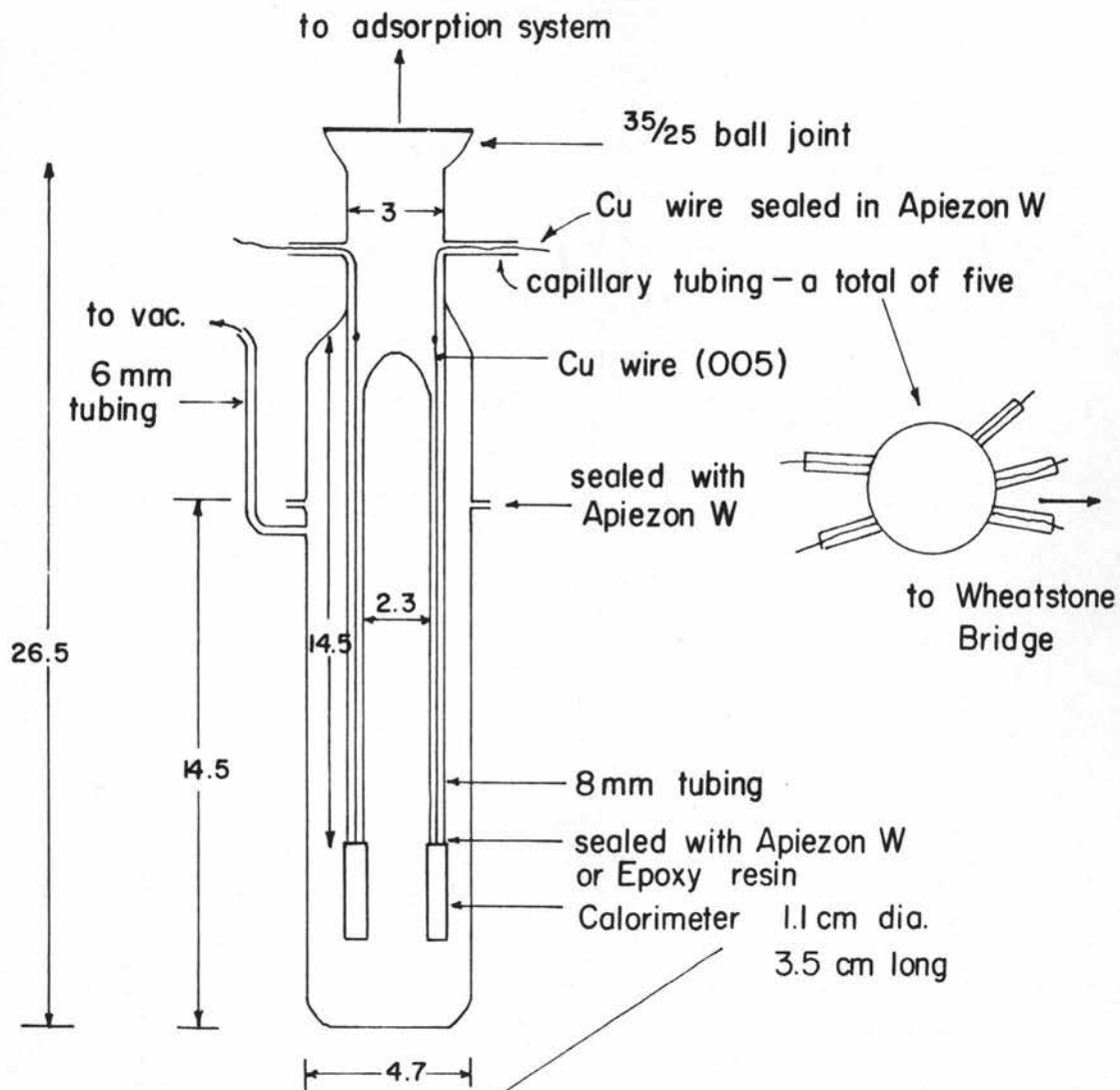
Another major source of error was that in order to adsorb quantities of  $\text{NH}_3$  above 180 mg./g., it was necessary to increase the pressure above atmospheric. Hence, while the diffraction was being made, some  $\text{NH}_3$  did escape, which could not be prevented. This was eliminated somewhat by cooling the sample before breaking the tube (B) and making the diffraction. However, the values shown in Figure 13 do not show the true weight of  $\text{NH}_3$  adsorbed on the sample, but only the maximum possible amount adsorbed.

#### Measurements of the Heats of Adsorption

Apparatus. The calorimetric apparatus used to measure heats of adsorption is shown in Figure 5. It is similar in certain respects to the calorimeter used by Beebe et al (6,p.839) and to the type of calorimeter suggested by Dressel (26,p.1-14). In order to eliminate the effects of compression, adsorption on

Figure 5

Calorimetric Assembly for the  
Measurement of Heats of Adsorption

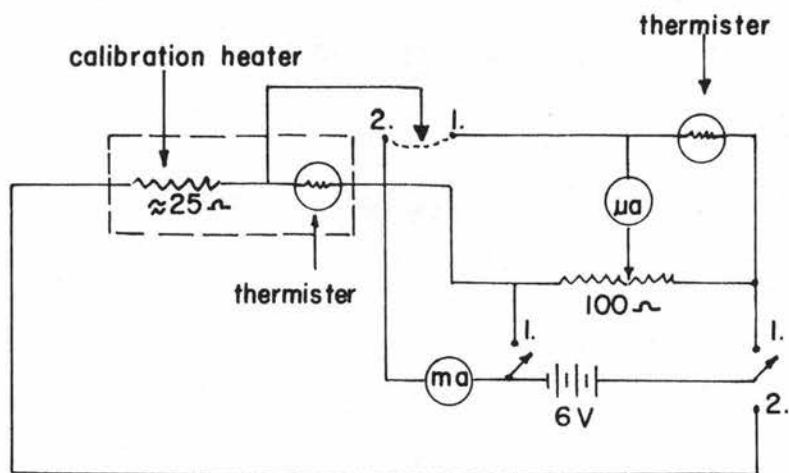


calorimeter walls and other extraneous heat losses or gains, twin calorimeters were used.

The calorimeters were made of 0.005 inch rolled electrolytic copper sheeting. The copper was fitted into the shape of a bucket and soldered well enough to withstand an internal pressure of 15 psi. Both calorimeters were of the same approximate weight and area. The calorimeters were mounted to the glass inlet tube with Apiezon W wax. Extreme caution had to be taken when the calorimeters were mounted to avoid leakage and to avoid getting the sample too hot when the wax was heated. Copper fins were placed inside the calorimeter and through the sample to insure better heat conduction.

The temperature detectors were matched Western Electric thermistors, model 17A. The approximate resistance at 0°C was 3,300 ohms, and their temperature coefficient of resistance was -4.4% per degree. The resistance of the two thermistors varied from each other approximately 1% in 25°. These thermistors were placed in the arms of a wheatstone bridge circuit as shown in Figure 6. The change in the temperature was determined by measuring the off-balance current between the thermistor in the sample and the one in the dummy

Figure 6  
Wheatstone Bridge Circuit for Measuring  
Temperature Change in Calorimeter



calorimeter with a milliammeter, or a nine millivolt Varian recorder.

In order to avoid the determination of the heat capacity of the system, a calibration heater was placed in the calorimeter containing the sample. The heater was constantan wire (005) with a resistance of 11.6 ohms per foot wrapped around the copper fins inside the calorimeter. The total resistance was usually around 25 ohms. Since the heaters were quite fragile, it was sometimes necessary to replace them frequently. Current from a six volt battery was sent through the heater for an arbitrary number of seconds measured by a stop watch. The amount of current was measured by a Heathkit milliammeter and could be read to  $\pm 1$  milliamp, (approximately 0.8%). The heat added to the system was then calculated from the equation:

$$(12) \quad Q = Ri^2t/4.18$$

where  $i$  is the current in amperes;  $t$  is the time in seconds;  $R$  is the resistance of the calibration heater; and 4.18 is the conversion factor for joules into calories.

Procedure. A sample of graphite oxide was tamped into the previously weighed calorimeter around the

fins and heater, after which the filled container was again weighed. Usually about one gram of sample was used. The calorimeter with its wire leads was then mounted on the glass tubing. Before mounting, however, the leads were soldered to wires running down through the tube from the outlets at the top of the glass container (see Figure 5). As the calorimeter was being mounted, these wires were pulled snug from the top with tweezers. Then hot wax was rubbed around the outer edge of the glass tubing, and the calorimeter (slightly larger in diameter) was shoved over the tube until it touched the fins, leaving approximately 1/8 inch lip extending over the tube. The wax was then allowed to cool and harden. The twin calorimeter was mounted in the same fashion.

Next the calorimeter was attached to the vacuum system used in the adsorption runs by the ball joints shown in the figure. The vacuum jacket was evacuated at the same time as the sample in the calorimeter, which was outgassed in the same manner as in the adsorption runs. After the sample was outgassed, the vacuum chamber was sealed from the rest of the system by closing a stopcock, leaving a hard vacuum in the jacket of less than 0.1 micron pressure.

The calorimetric system was then submerged in a Dewar flask filled with an ice - water bath which was kept agitated with a stirring motor. The temperature of the system was allowed to come to equilibrium overnight; the next morning an appropriate increment of ammonia was added to the system. The off-balance current was measured at half minute intervals in the beginning of the run to increasing intervals of five or ten minutes at the end of the run when the temperature returned to  $0^{\circ}\text{C}$ .

At the end of each run heat was added to the system by means of the calibration heater described above. Here again the current-time data was taken as before. When the original temperature was reached, another increment of ammonia was added, and the procedure was repeated.

It usually took between three-fourths to one and a half hours for the temperature to come back to  $0^{\circ}\text{C}$  during the adsorption. Some residual adsorption took place after this time, but the heat was too small to be detected. In the calibration of the calorimeter the system came back to equilibrium in about one half hour.

The time-current data were plotted on vellum paper,

and the graphs were cut out and weighed on an analytical balance. The weight of the graph from the absorption run was compared to that obtained from the calibration run. The heat of adsorption was determined from the ratio of the weights of the two graphs and from the known heat input in the calibration run. This procedure is not as accurate as calculations by numerical integration methods, but it is not nearly as time consuming. Approximately a 3% error could be estimated for this method because of the difference in the density of the paper.

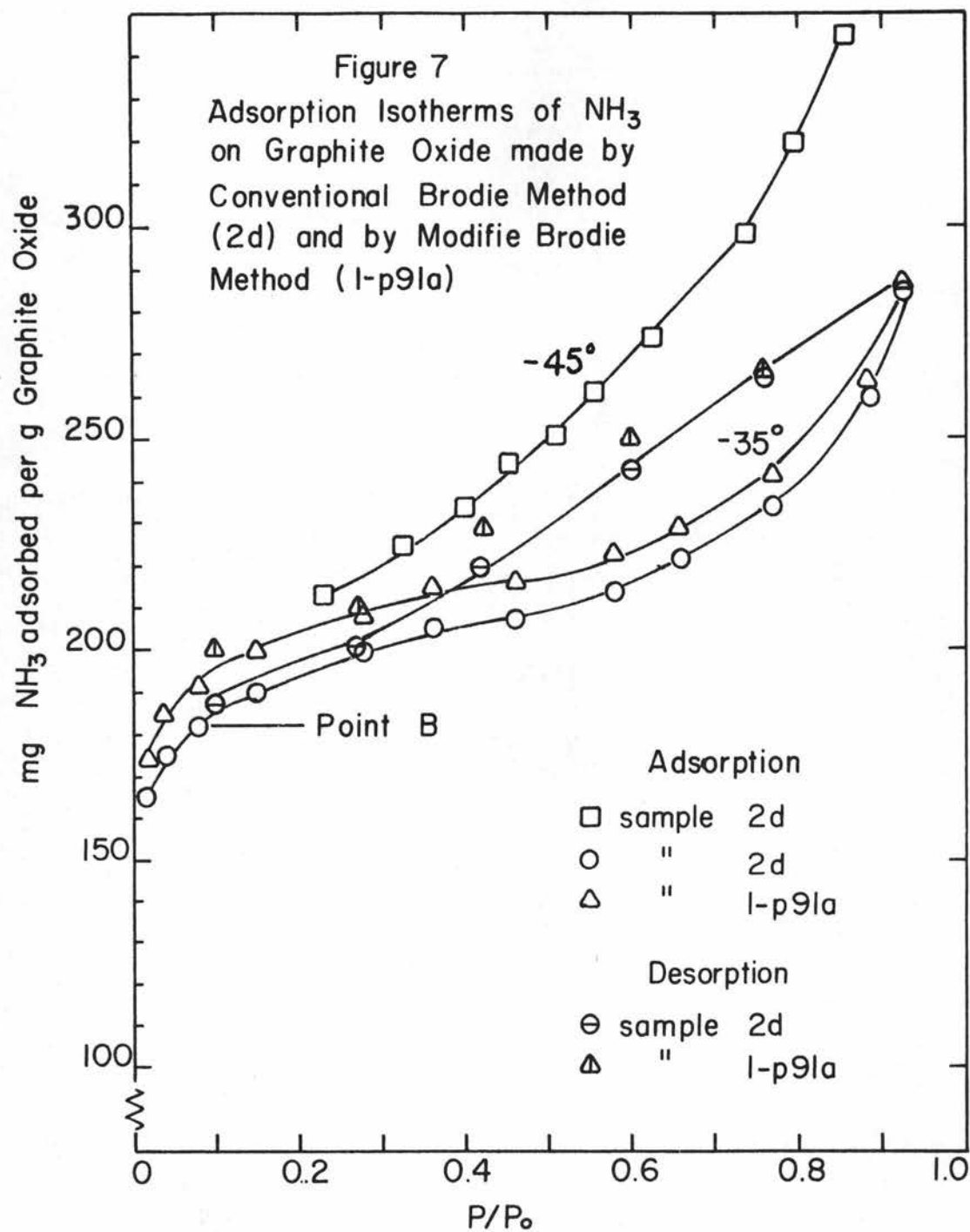
In order to determine the weight of the  $\text{NH}_3$  adsorbed per gram of graphite oxide, another sample was subjected to the same conditions as that in the calorimeter. This sample was suspended from a spring balance used in the determination of isotherms, and the change of weight was followed in the same manner. The column housing the spring and sample were attached to the same adsorption system as the calorimeter; therefore, the two samples were under exactly the same pressure.

## DISCUSSION OF EXPERIMENTAL RESULTS

Adsorption Isotherms

Graphite oxide. Adsorption isotherms were obtained for graphite oxide samples, 2a, 2b, 2c, and 2d, at  $-45^{\circ}$ ,  $-36^{\circ}$  and  $-25^{\circ}$ . The isotherms for the four samples were almost identical in shape, although their vertical displacement varied over a range of six per cent. There was also relatively little difference between the isotherms obtained at  $-36^{\circ}$ ,  $-35^{\circ}$ , and  $-25^{\circ}$ . Because of the similarities mentioned above, only the isotherms for sample 2d are shown in Figure 7 for  $-45^{\circ}$  and  $-35^{\circ}$ . An isotherm of sample 1-P58a at  $-35^{\circ}$  is also shown in Figure 7 demonstrating that there is little difference in isotherms of graphite oxide made by the conventional Brodie method and graphite oxide made by the modified Brodie method.

The curves shown in Figure 7 tend to follow a type 1 and type 2 isotherm. The rapid adsorption of  $\text{NH}_3$  at low pressures indicate that a monolayer of  $\text{NH}_3$  is formed easily and rapidly, while the second layer is relatively more difficult to form. The constancy of the "point B" (even at  $+25^{\circ}\text{C}$ ) relative to  $P/P_0$  indicates that the mechanism of the adsorption



tends to hinge on some type of condensation effect.

The data obtained from the isotherms gave linear plots for the B.E.T. equation up to a partial pressure of approximately 0.18. Ordinarily the B.E.T. equation is good up to a partial pressure up to approximately 0.35; however, the initial uptake of  $\text{NH}_3$  on graphite oxide is so high that a monolayer is formed at relatively low relative pressure in comparison with other systems. Therefore, with this in mind, it would seem logical that the B.E.T. equation would not cover such a large range in the present case. No significance can be given to the fact that the B.E.T. plot extrapolates to zero.

Figure 8 shows a B.E.T. plot which is representative of those obtained for samples at both  $-45^\circ$  and  $-36^\circ$ . The surface areas of the samples were calculated from information obtained from these plots; the calculations were based on an area for the  $\text{NH}_3$  molecule of  $12.9 \text{ \AA}^2$ , which was obtained from equation 4. The areas shown in Table 2 are much higher than the  $358 \text{ m}^2/\text{g}$  observed by De Boer and Van Doorn (11, p.242-252) for the adsorption of water vapor. De Boer and Van Doorn calculated the theoretical surface area for both sides of the lamellar platelets of graphite oxide.

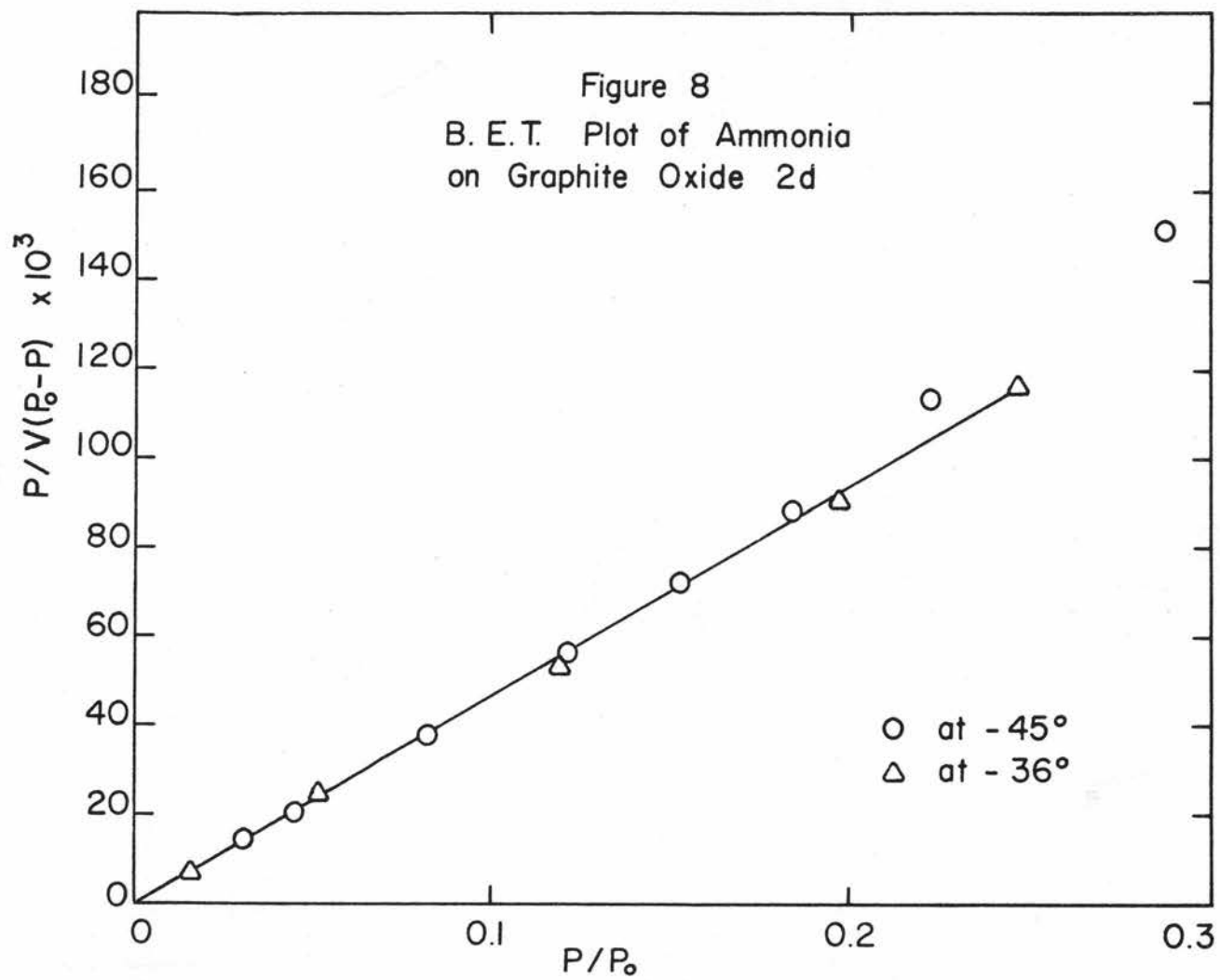


TABLE 2

SUMMARY OF ADSORPTION BEHAVIOR  
OF GRAPHITE OXIDES AND SALTS

	Graphite Oxide at $-36^{\circ}$				Graphite Oxide Salts at $-35^{\circ}$			
	2a	2b	2c	2d	Li	Na	K	Rb
$W_m$ - B.E.T. (mg./g.)	164	170	175	167	142	143	144	144
Meq./g.	9.7	10.0	10.3	9.8				
Area ( $m^2/g.$ )	750	778	799	764	649	657	658	658
Residual $NH_3$ after desorption at $25^{\circ}$								
mg./g.	42.3	42.8	34.6	35.1	47.9	--	33.8	31.4
meq./g.	2.49	2.52	2.04	2.06	2.82	--	1.98	1.85
Residual $NH_3$ after desorption at $70^{\circ}$								
mg./g.	--	21.7	13.4	13.8	42.8	--	27.4	25.0
meq./g.	--	1.28	0.79	0.81	2.52	--	1.61	1.47

Their calculated value of  $1477 \text{ m}^2/\text{g}$ . is on the average  $180 \text{ m}^2/\text{g}$ . lower than the values obtained by doubling the  $\text{NH}_3$  area in Table 2. The area found experimentally would consist of the area of only one side of the platelets plus the area on the outer surfaces (area found from  $\text{N}_2$  isotherms); therefore, these values doubled should be approximately  $160 \text{ m}^2/\text{g}$ . larger than the theoretical area calculated by De Boer and Van Doorn, which is in good agreement with what is found.

The break in the isotherm ("point B") appears at approximately  $175\text{-}180 \text{ mg. NH}_3/\text{g.}$ , which is in very good agreement with the  $W_m$  calculated by the B.E.T. equation. The  $\text{meq./g.}$  of  $\text{NH}_3$  adsorbed at this point corresponds quite closely to the value,  $11.0$ , obtained by Clauss et al (22,p.205-220) for the exchangeable hydrogen by methods previously mentioned. This correspondence is probably only coincidence, but if it were not for the closeness to the theoretical area there would be some doubt in the validity of the experimental areas since the isotherms could very well be gaseous titration curves for ion exchange sites.

Hysteresis loops were found when the samples

at  $-36^{\circ}$  and  $-35^{\circ}$  were outgassed. The hysteresis tended to close at a partial pressure of approximately 0.2 in some cases and then seemed to open again at lower pressures. An attempt to explain this phenomena will be made later.

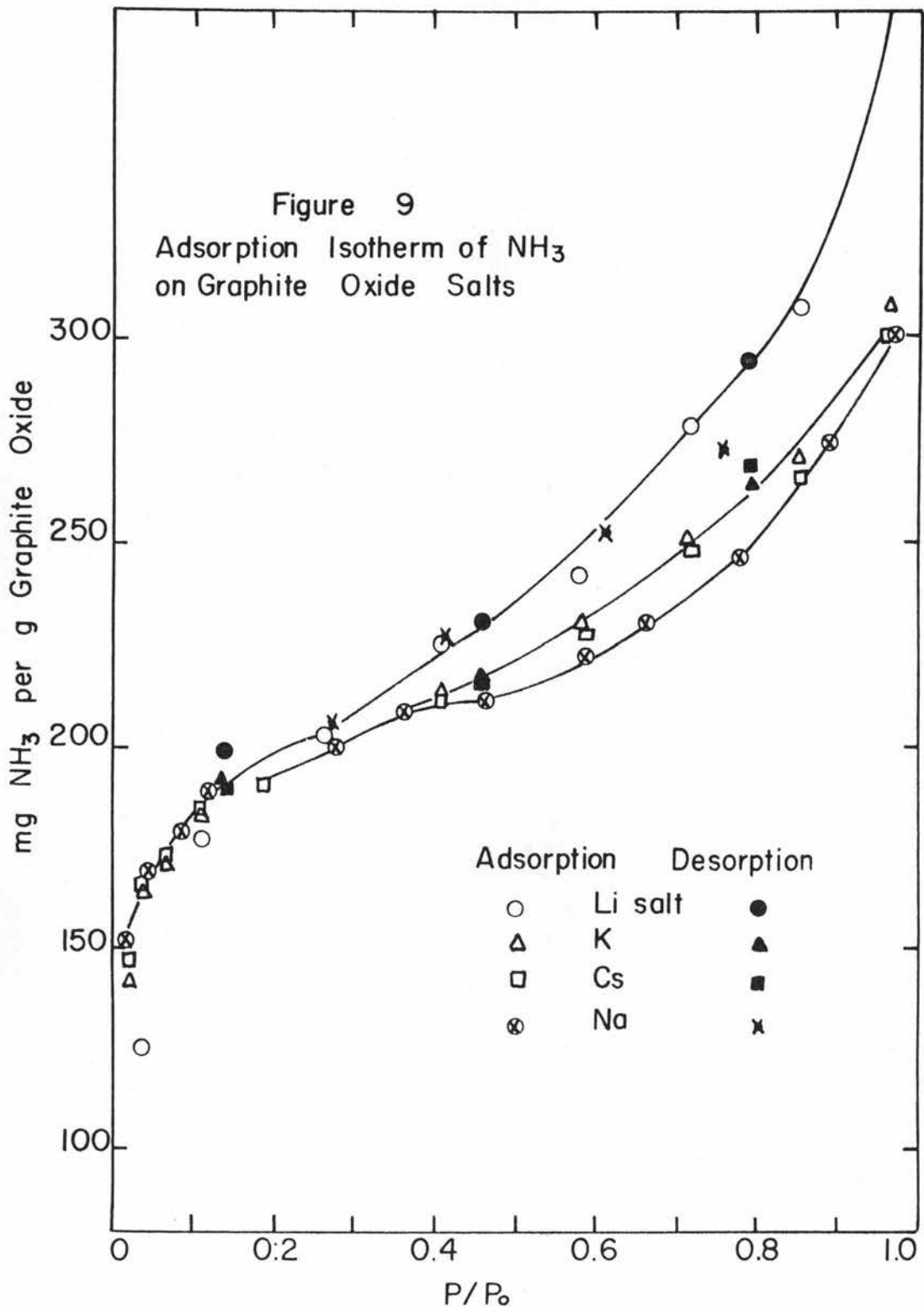
The samples could not be completely desorbed even after outgassing for six days at less than one micron pressure. The weights of  $\text{NH}_3$  left are shown in Table 2. These values were lowered, as also shown in the table, by heating the samples to  $70^{\circ}\text{C}$ . Higher temperatures were not used because it was feared at the time that decomposition would take place.

Incomplete outgassing in adsorption systems have been noted by other investigators in the literature. Zettlemyer et al (81,p.375) noticed this phenomena on the outgassing of  $\text{NH}_3$  from stearic and succinic acids. Since they found one half the stoichiometric equivalents of  $\text{NH}_3$  per equivalent of carboxyl groups remained adsorbed at room temperature, they suggested that a semi-stable complex was formed,  $\text{RCOOH} \cdot \frac{1}{2}\text{NH}_3$ . If this were true with carboxylic groups on graphite oxide, then twice the number of meq. shown in Table 2 at  $25^{\circ}\text{C}$  should be approximately the number of carboxylic groups present in graphite oxide (4.1 to 5.0 meq./g.).

Cornet in his studies with  $\text{NH}_3$  on Montmorillonite clays found that on outgassing hydrogen bentonite the residual  $\text{NH}_3$  corresponded to the exchange capacity of the clay. He postulated that this  $\text{NH}_3$  was left in the form of  $\text{NH}_4^+$  ion, where  $\text{ROH} + \text{NH}_3 \rightarrow \text{RO}^-\text{NH}_4^+$ . If this were the case then the number of readily exchangeable hydrogen ions in graphite oxide would be between 2.04 to 2.52 meq./g.

There is another possible reason for incomplete outgassing that should not be overlooked. If graphite oxide is tautomeric as previously discussed, then when the compound is in either the enol or keto state, there will be "holes" in the lattice as demonstrated in Figure 1 b where a carbon to carbon bond is disrupted. It is reasonable to believe that, because of the tetrahedral configuration of carbon compounds, these openings would not be filled by either the oxygen or the hydroxyl group. If this is the case, it would be possible for  $\text{NH}_3$  to fill these openings and to become trapped there as the platelets collapsed upon outgassing.

Graphite oxide salts. The graphs for the adsorption of  $\text{NH}_3$  at  $-35^\circ$  by graphite oxide salts (Li, Na, K, and Rb) are shown in Figure 9. The isotherms



for all the salts except Na indicate very little hysteresis on desorption. The isotherm for Na graphitete has a relatively large hysteresis loop with the adsorption curve slightly lower than those for K and Rb and the desorption curve slightly lower than the adsorption curve for Li graphitete. It is concluded from the relative positions of these curves that true equilibrium for the adsorption of  $\text{NH}_3$  on the Na salt was not achieved.

The B.E.T. equation was applied to these isotherms, and the results are shown in Table 2. The areas are lower than for the graphite oxide in general. This is understandable in view of the fact that the metal ions require more space in the lattice than the hydrogen ions.

The weights of  $\text{NH}_3$  left on the samples after outgassing for three days at less than  $0.1\mu$  pressure are also shown in Table 2. These weights are similar to the weights retained by graphite oxide at  $25^\circ$ . No apparent reasons can be advanced regarding the larger retention of  $\text{NH}_3$  by the salts at  $70^\circ\text{C}$  or the larger retention of  $\text{NH}_3$  on Li graphitete than on the K or Rb salt. If it is assumed that the metal ions replace all the hydrogen ions on the carboxylic acid groups,

then the theories proposed in the section on the adsorption isotherms of graphite oxide regarding the retention of  $\text{NH}_3$  on ion exchange sites or as  $\text{NH}_3$  complexes must be discarded. The indication is that on the outgassing of the samples, the platelets collapse together trapping  $\text{NH}_3$  molecules within the lattice. This leaves the possibility that the metal ions may be large enough to fill in or close capillaries within the lattice when the platelets collapse, thus, trapping the  $\text{NH}_3$  which normally would escape at  $70^\circ\text{C}$ . This mechanism is supported by the close relationship between the amount retained on the sample after outgassing and the number of metal ions exchanged for hydrogen (Tables 1 and 2).

Ordinarily hysteresis in adsorption isotherms are regarded as the result of capillary condensation within the particle. In this work the lack of hysteresis for the isotherms of graphite oxide salts seems to exclude this possibility. It indicates that hysteresis depends on the readily exchangeable acid groups in the sample. It is possible that formation of  $\text{NH}_4^+$  ions would cause hysteresis because of the high energy required to break these bonds.

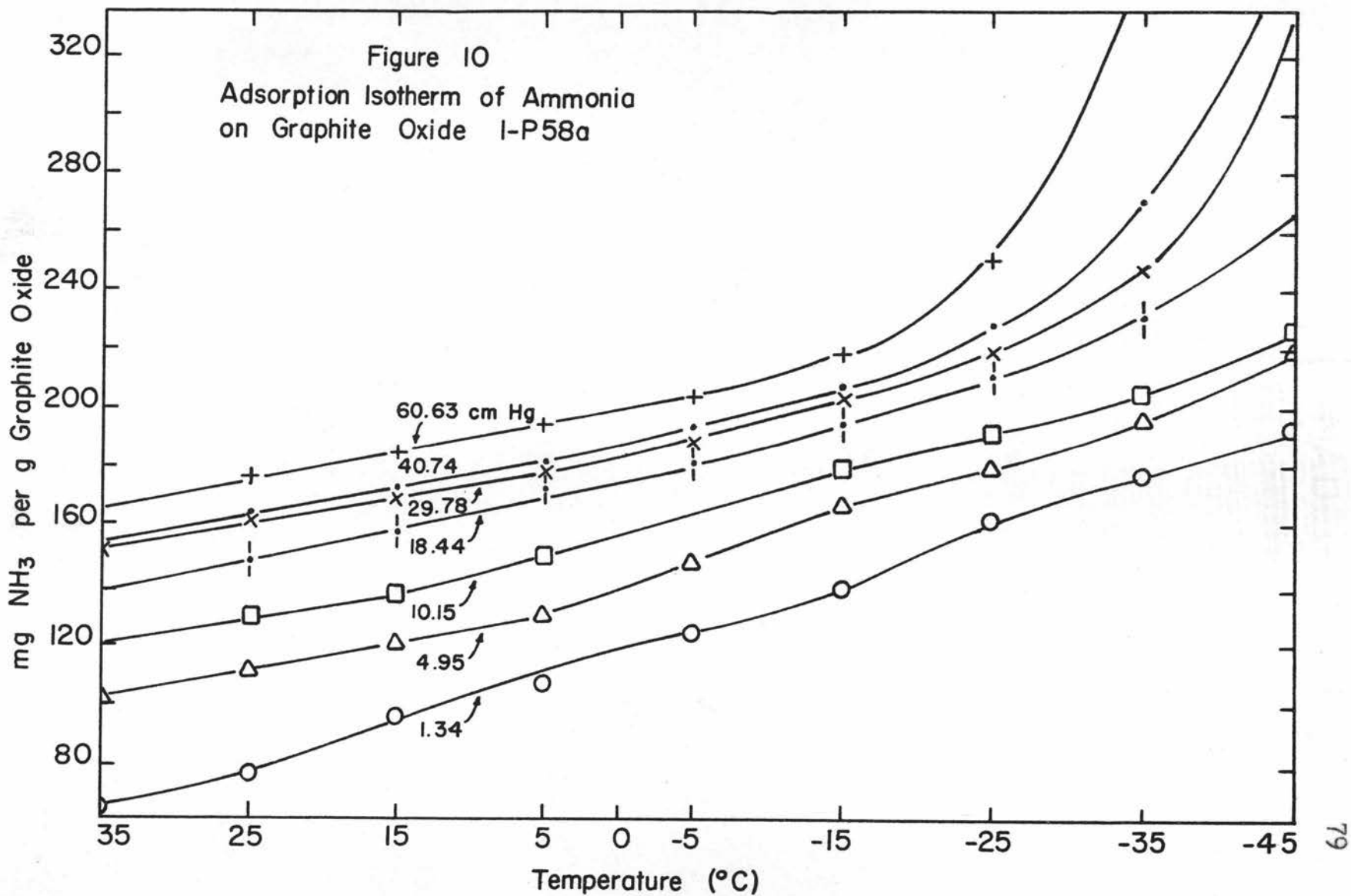
### Adsorption Isobars

Isobars in general. The adsorption isobars were obtained in order to calculate the isosteric heats of adsorption. Calculation of isosteric heats is also possible from the isotherms; however, in this case it is difficult to calculate them accurately in the region at "point B" because the isotherms at various temperatures are too close together. The isosteric heats and their interpretation will be discussed in another section.

The isobars are shown in Figure 10 where they cover a range from  $35^{\circ}\text{C}$  to  $-45^{\circ}\text{C}$ . From the curves, it can be seen that the adsorption may be considered a linear function of the temperature until one reaches higher pressure. The increase of adsorption with the decrease in temperature is a good indication that the process is at least partially physical. Unfortunately the isobars were not obtained for higher temperatures; however, at the time, it was feared that decomposition might take place since graphite oxide may be unstable in the presence of ammonia and amines at higher temperatures (63,p.43-56).

Isosteric heats. The isosteric heats were calculated from the isobars with the Clausius-Clapeyron

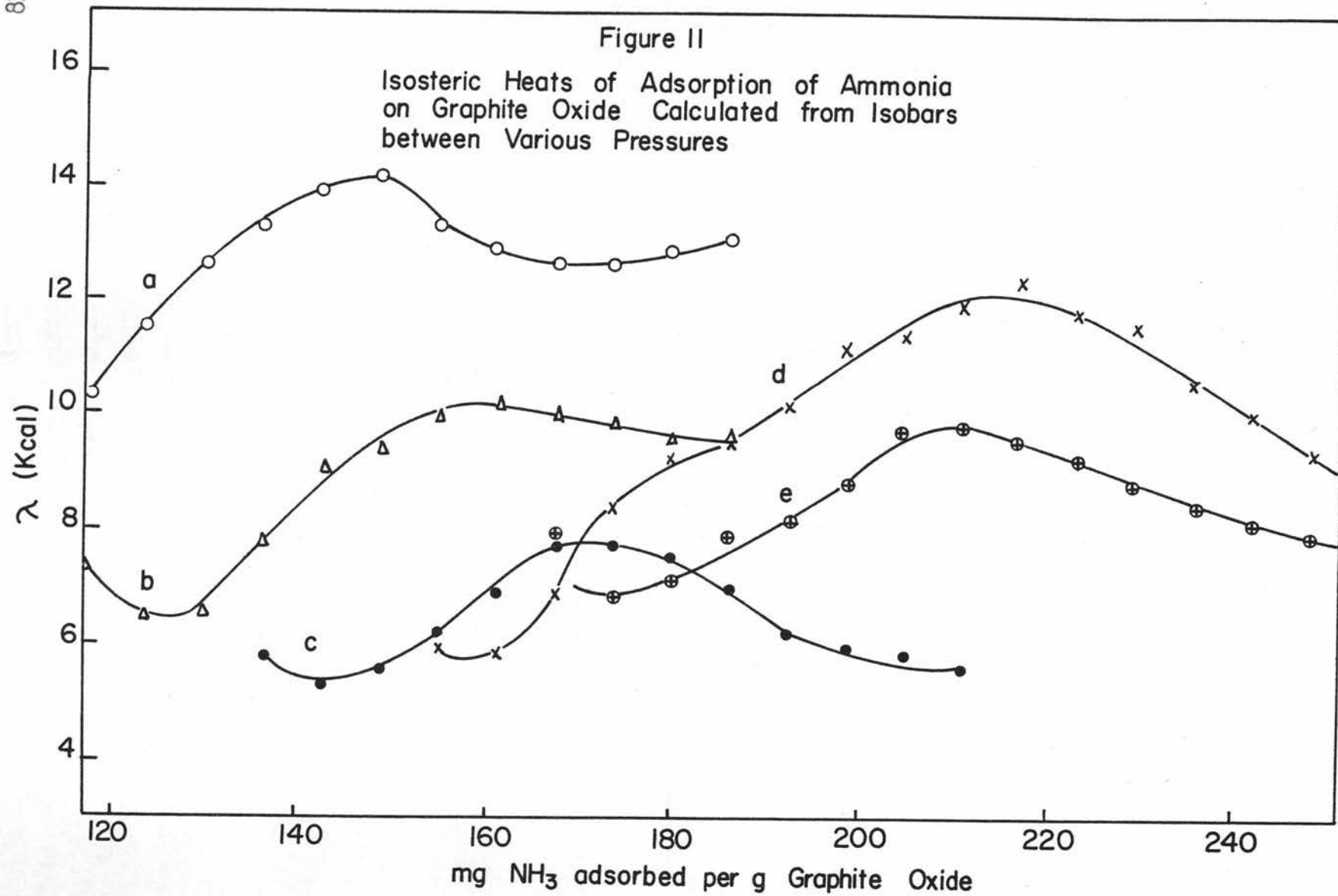
Figure 10  
Adsorption Isotherm of Ammonia  
on Graphite Oxide I-P58a



equation (Equation 11). There is some controversy on the validity of the use of the Clausius-Clapeyron equations on non-reversible systems such as the graphite oxide -  $\text{NH}_3$  system. Therefore, we shall consider the values only as apparent isosteric heats. Yet it is quite likely that these apparent values are at least a qualitative representation of reality.

The isosteric heats are plotted in Figure 11 for different pressures. Contrary to what might be expected, none of the maxima of these curves correspond to the  $W_m$  value, nor do these peaks fall in that general region. Instead, both the position and magnitudes of the heats show a regular trend as the pressure is increased. Because of the shape of the isobars, these heats could be calculated only in the region where the monolayer is filled.

The isosteric heats are approximately in the same range as those found calorimetrically. However, since they are determined under a different set of conditions than the calorimetric heats, direct comparison of the two cannot be made. Interpretation of these results can only be made in view of the fact that the mechanism of adsorption will change somewhat at different pressure levels.



The general form of the curves suggests the following mechanism for the adsorption of  $\text{NH}_3$  by graphite oxide. Initial adsorption probably takes place on the outer edges of the platelets. High values should be obtained in this region because of the reaction of  $\text{NH}_3$  with the carboxyl groups which many workers believe to be situated on these edges. These values would appear in the region not measured by the isobars.

In the next phase, the platelets are mechanically pried apart by  $\text{NH}_3$  with a resultant decrease of heat energy. The subsequent adsorption takes place with increasing ease, and less energy is used in mechanically prying the layers apart. The heat curves show a continual increase with a maximum at the point where all the exposed sites are saturated. However, in graphite oxide the rigidity of the graphite structure is at least partially destroyed. Therefore, there are portions of the layers which remain collapsed until forced open by more adsorbate. Energy is used in the process, and the heat curves show a minimum in this region.

As the pressure increases, more gas is forced into the interlayer at once. This exposes a larger

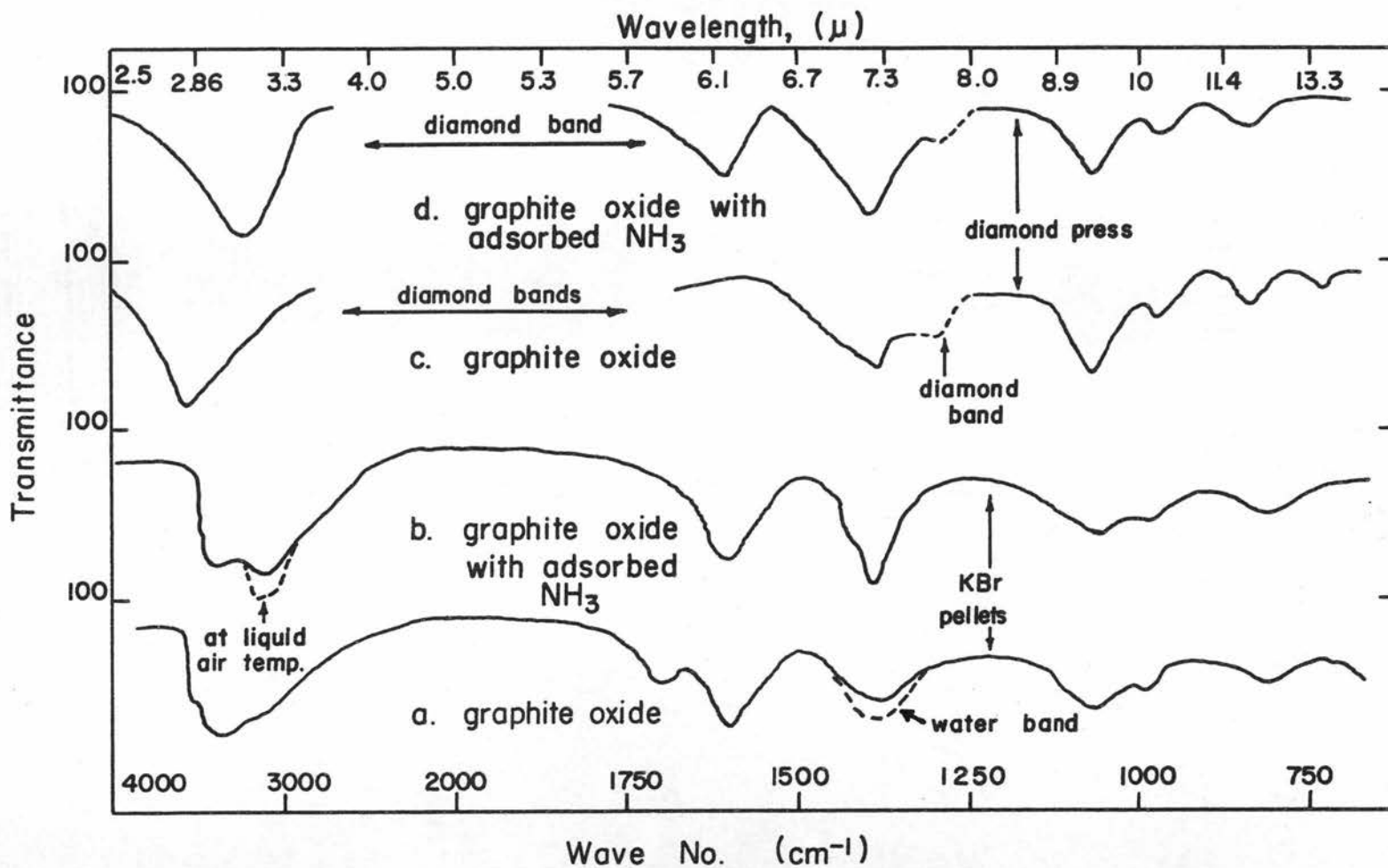
area and the heat curve maximum is shifted to higher weights adsorbed. In this process more over-all energy is used and there is a net decrease in heat.

At still higher pressures, the same mechanism remains in effect. However, in this region other factors must be considered, such as surface condensation, lateral interaction of  $\text{NH}_3$  molecules with each other in the completed monolayer, and the formation of additional layers; surface condensation and lateral interaction of  $\text{NH}_3$  molecules are probably responsible for the increase of net heat. This net heat decreases as the pressure increases due to the prying of the platelets still further apart in the formation of multilayers. It is reasonable to assume that this step would require considerable energy because of the possibility of some hydrogen bonding between the  $\text{NH}_3$  molecule and the active sites on the two adjacent platelets.

#### Infrared Absorption

The infrared absorption spectra of graphite oxide is characterized by a relatively broad band in the 3300 - 3500  $\text{cm}^{-1}$  region (Figure 12). According to Hadzi and Novak (31,p.1614-1620) the band in this

Figure 12  
Infrared Absorption of Graphite Oxide



region is due to the O-H stretching vibration for graphite oxide itself. A shoulder appears at approximately  $3250\text{ cm}^{-1}$  when the graphite oxide contains adsorbed water; the shoulder develops into a well-defined peak as the water content increases. This peak is clearly the result of the O-H stretching motion of the water molecule. In the present case, the band in this region retains some semblance of a shoulder even for samples dried at  $160^{\circ}\text{C}$  for three hours or dried under pressure of less than 0.1 pressure. It is very possible that enough moisture was adsorbed from the atmosphere to show some traces of water. Hadzi and Novak do not describe their method of treating the sample after drying, so it is not known if the samples were run in an inert or dry atmosphere.

A well defined shoulder also appears at  $3250\text{ cm}^{-1}$  for graphite oxide with adsorbed  $\text{NH}_3$  (Figure 12b) at room temperature. This peak was intensified considerably by cooling the sample to liquid air temperatures and using a LiF prism. The assignment of this band may be made to the hydrogen stretching motion (N-H) from either the ammonium ion or to  $\text{NH}_3$ , itself. (57, p. 1059-1062). The band is too diffuse to distinguish between any respective bands.

The spectrum obtained from vacuum dried graphite oxide compressed between diamond crystals shows a relatively sharp peak at  $3530\text{ cm}^{-1}$ . This peak was shifted to a lower frequency,  $3250\text{ cm}^{-1}$ , upon the adsorption of  $\text{NH}_3$ . The shift may be caused by hydrogen bonding of  $\text{NH}_3$  with a hydroxyl group. The band at this frequency is a little broader, which might mean that it is a combination of two peaks, although the intensity is approximately the same.

The small band at  $1720\text{ cm}^{-1}$  may be assigned to free carboxylic carbonyl groups. This agrees with findings of Hofmann and Holst (36,p.754-771) in that graphite oxide has carboxylic acid groups. The adsorption of  $\text{NH}_3$  either destroys this band or shifts it to a region already masked by another band, such as the region near  $1610\text{ cm}^{-1}$  or the  $1375\text{ cm}^{-1}$  region. It is believed that a band shift is most probable because of the formation of an ammonium salt. Strangely enough, this band does not appear in the spectrum obtained from graphite oxide pressed between the diamond crystals. It is possible that the high pressures used in compressing the sample are enough to destroy these groups since it is known that graphite oxide will decompose under certain conditions when ground in a mortar and pestle (74,p.1-20).

The sharp band at  $1610\text{ cm}^{-1}$  was present in every spectra obtained from graphite oxide using the pressed salt technique. This peak seemed unaffected in any way by the adsorption of  $\text{H}_2\text{O}$ ,  $\text{SO}_2$  or  $\text{NH}_3$ . However, Hadzi and Novak found this peak only in wet graphite oxide. It did not entirely disappear even after a week of drying over  $\text{P}_2\text{O}_5$  under high vacuum. In this work it was found that the peak seemed just as intense with graphite oxide dried at three hours at  $160^\circ\text{C}$  as for wet graphite oxide. As mentioned above, it is possible that sufficient moisture was picked up from the atmosphere to give a peak in this region. However, there is a question of why this peak does not increase in intensity with increased moisture content.

The spectrum obtained from the oxide compressed between diamond did not show a peak in the  $1610\text{ cm}^{-1}$  region; however, one appears with the adsorption of  $\text{NH}_3$ . This band may be assigned to the unsymmetrical bending vibration of  $\text{NH}_3$ .

Hadzi and Novak assign the band at approximately  $1400\text{ cm}^{-1}$  to the deformation mode of O-H groups. This is most probable because this band is intensified with adsorbed water. It is also intensified to a larger degree with adsorbed  $\text{NH}_3$ . According to Pliskin

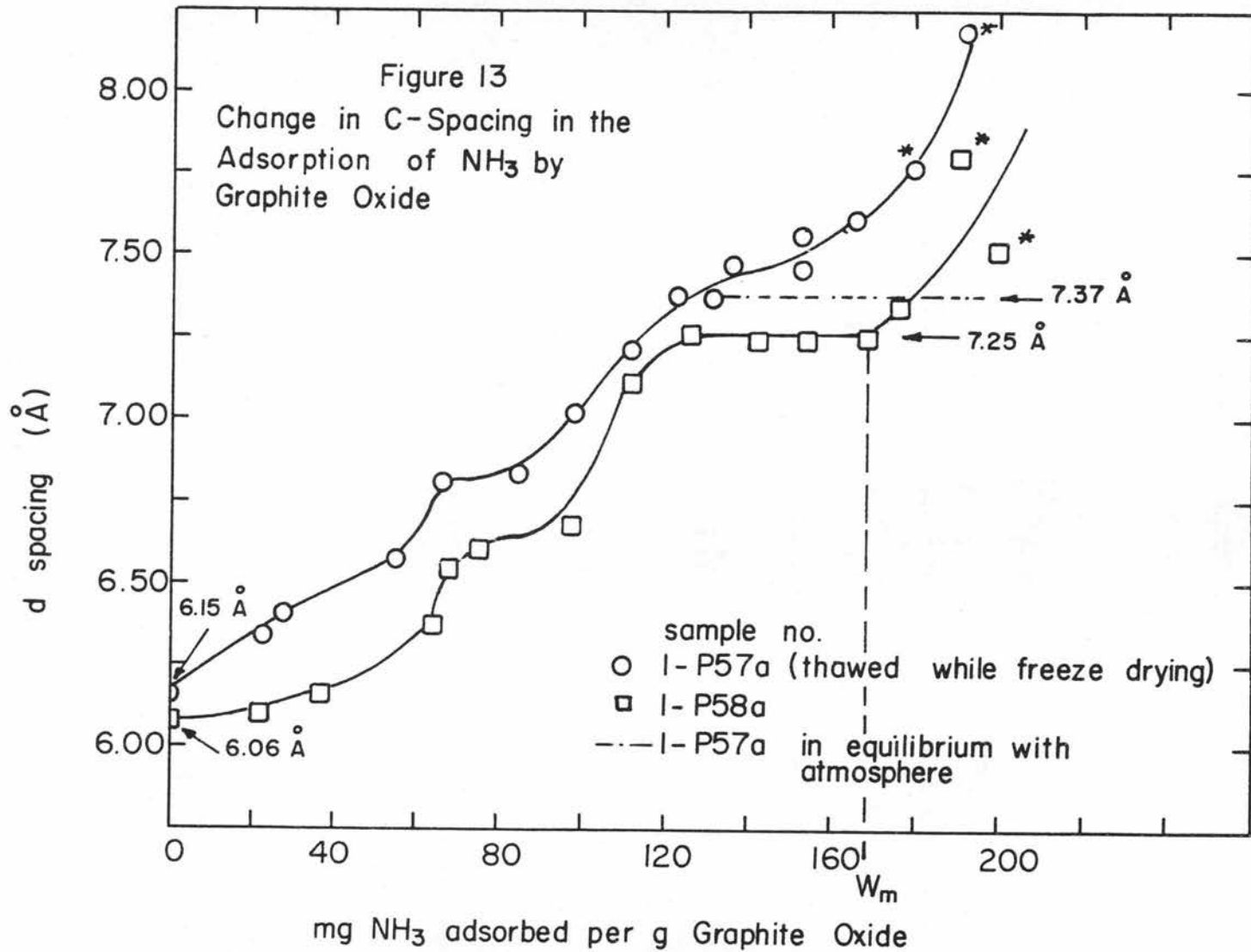
and Eischens (62,p.1156-1159) there is an appearance of a band in the  $1400\text{ cm}^{-1}$  region due to the N-H bending vibration of the ammonium ion which has exchanged with potassium ion in the KBr pellet. However, this is unlikely in this case because the KBr and graphite oxide were mixed after the adsorption took place. Also, this band shows an increase of intensity in the spectrum obtained from the graphite oxide compressed between diamond. Therefore, this band can be attributed to the formation of  $\text{NH}_4^+$  ions in the oxide.

The other bands at lower frequency show no change upon the adsorption of  $\text{NH}_3$ . These bands are intensified somewhat in the spectra obtained with the diamond press and by cooling the samples down to liquid air temperatures. There is one small band ( $740\text{ cm}^{-1}$ ) which appears in Figure 12c and which disappears in the spectrum in Figure 12d. There is a slight indication of this band in Figure 12a. Absorption in this region may be due to the skeletal vibrations of the solid lattice. This could explain the disappearance of this peak upon adsorption of  $\text{NH}_3$ . The  $\text{NH}_3$  in between the graphite oxide platelets would change the nature of the lattice and influence its vibration frequency, causing the band to shift.

From information obtained in these studies certain facts are indicated. Ammonium ions are formed upon adsorption of  $\text{NH}_3$  on graphite oxide. The hydrogen on the adsorbed  $\text{NH}_3$  is not necessarily bonded to any oxygen groups; however, there still remains the possibility that hydrogen from graphite oxide may be bonded to the nitrogen atom, as this does not necessarily influence the position of the N-H bending or stretching bands (69,p.6159-6163). There is a possibility that there may be some significance to the fact that  $\text{NH}_3$  does not influence the absorption bands between  $1250 \text{ cm}^{-1}$  to  $750 \text{ cm}^{-1}$ . These bands have been assigned by Hadzi and Novak to oxygen containing groups, such as C-O, O-H, epoxy, and even the possibility of some hydroperoxides. Any hydrogen bonding between the  $\text{NH}_3$  and the oxygen should have some effect on the position of the peaks. Adsorption spectra of graphite oxide itself indicate the possibility of hydrogen bonding between hydroxyl and oxygen groups within the graphite oxide layers.

#### X-Ray

The change of the (001) or c-spacing of graphite oxide in relation to the amount of  $\text{NH}_3$  adsorbed is shown in Figure 13. No actual reason can be given for



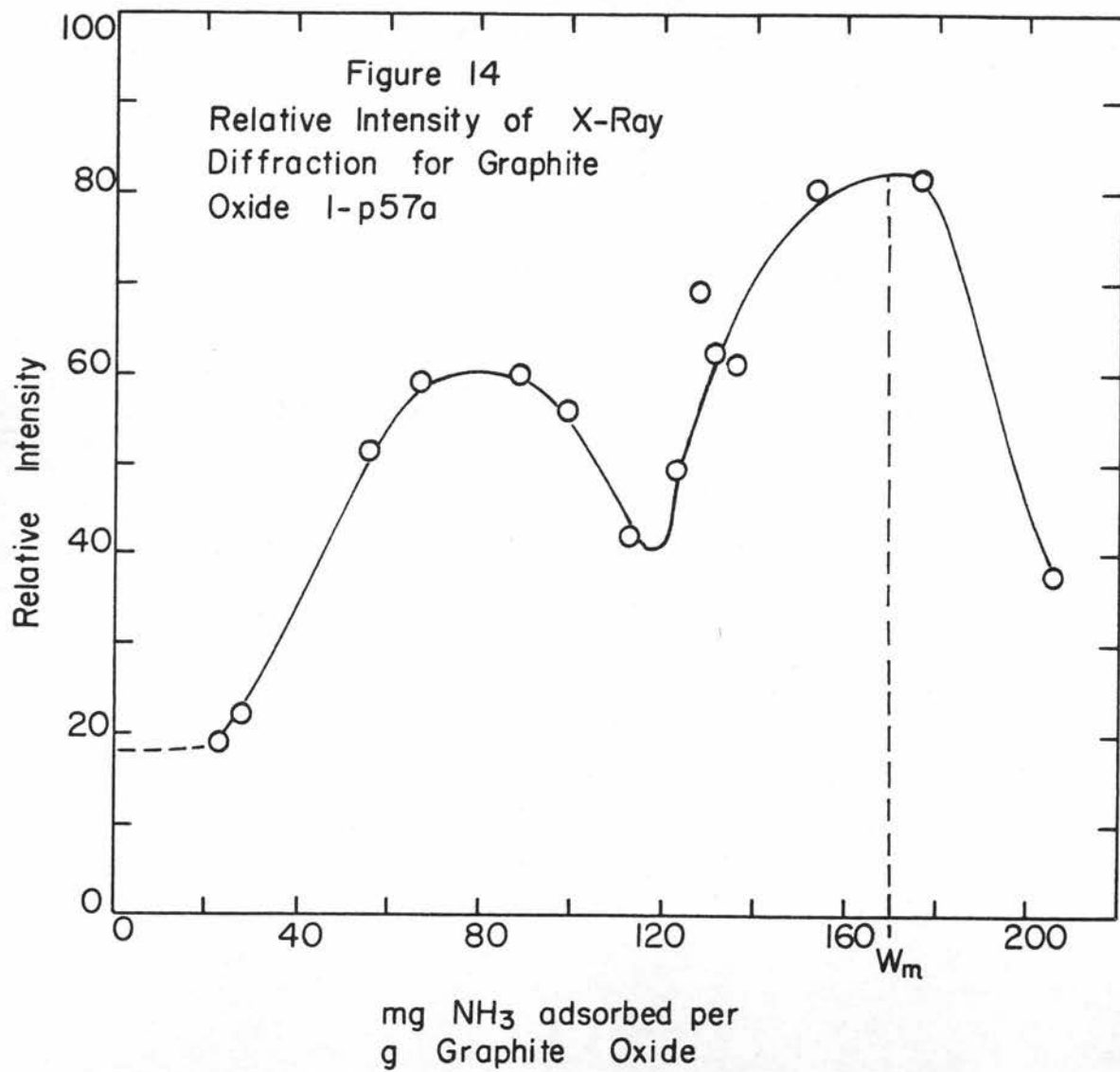
the discrepancy between the two graphs shown in the Figure. It is possible that the difference in freeze drying of the two samples may have had some effect in the orientation of the atoms or groups of atoms in the graphite oxide structure which would change the c-spacing. There is also the possibility that sample 1-P57a may not have been completely dry before adsorption took place, and that a slight amount of moisture may have altered the structure of graphite oxide platelets. However, the latter is not likely because several experiments indicate the same magnitude for the c-spacing of each sample used.

Three major breaks occur in both curves at 67, 122 and 175 mg. of  $\text{NH}_3$  adsorbed per gram of sample. The difference in c-spacing for the minor plateaus is 0.57 A for sample 1-P58a and 0.65 A for sample 1-P57a; for the major plateaus, the values are 1.19 A and 1.22 A respectively. These latter values may be considered as the distances the platelets were expanded by a monolayer of  $\text{NH}_3$ . The c-spacing for  $\text{NH}_3$  saturated graphite oxide always decreased on exposure to the atmosphere to the constant value of 7.37 A for sample 1-P57a. It may be gathered that the graphite oxide expelled the excess  $\text{NH}_3$  until only a monolayer remained. This indicates that the force of attraction between

the graphite oxide platelets and the  $\text{NH}_3$  monolayer is quite large probably because of hydrogen bonding.

While no attempt was made to measure the relative intensity of the reflected X-rays, it was interesting to note that in every case the maximum intensity was obtained at 175 mg./g. A qualitative estimation of the relative intensities of sample 1-P57a is shown in Figure 14. This graph also shows a smaller maximum at 80 mg./g. which corresponds quite well with the first plateau in Figure 13. However, not all experiments showed such a well-defined peak at this point. Care must be taken in any analysis of this graph because the intensity may be influenced by other factors such as the thickness of the sample layer, distance of sample from polyethylene covering, and any variation of the thickness of polyethylene itself. Therefore, the only certain significant conclusion in this respect is that maximum intensity was obtained at 175 mg./g. or  $W_m$ . This fact would follow logically that one probably obtains the highest degree of crystallinity in the sample at this point.

It may be significant also that the dried ammonia-free samples and samples with relatively little ammonia adsorbed on them always had the lowest intensity and



were the most diffuse in a particular run. This phenomena could be accounted for in two ways. One, the atoms in a layer are relatively diffuse; that is, they are oriented in no particular plane, and, therefore do not show the full properties of a crystalline material. Second, if graphite oxide has the warped structure as shown in Figure 1A, there would be two planes of carbon atoms approximately 0.5 Å apart. The X-ray beam reflecting from the second plane would be slightly out of phase with that reflecting from the top plane. This would cause interference and diminution of the intensity and resultant amplitude.

The stepwise X-ray curves have also been found in other systems, particularly in the studies of clays (24,p.217-226)(82,p.962-966). However, plateaus were always attributed to the respective formation of layers of adsorbate between the adsorbent platelets. In the present case only the plateau starting at 122 mg./g. of graphite oxide may be considered as corresponding to a single layer formation; the other plateau is caused by some other phenomena for which an explanation will be attempted in the next paragraph. De Boer and Van Doorn (11,p.242-252) in their X-ray diffraction studies of graphite oxide with adsorbed water found very little

change in c-spacing until the sample contained over 16.2 per cent water (162 mg./g.). If one compares the calculated area of  $\text{NH}_3$  (12.9 A) to that of water (10.8 A) the 162 mg./g. would roughly compare with the 122 mg./g. in Figure 13 where the least change in c-spacing is found. They found that the c-spacing had at least expanded to 6.8 A from the 6.3 A. However, these investigators, from their calculations, claimed that this expansion was insufficient to account for all the adsorbed water, indicating that an adsorbed molecule may fit into the graphite oxide lattice without much effect on c-spacing.

According to Cano-Ruiz and MacEwan (19,p.227-242) in their review of the model of graphite oxide proposed by Ruess: The carbon atoms in a tetrahedral "chair" configuration will form two layers with a perpendicular separation of 0.5 A; the oxygen atom in the ether linkage will extend out from the center of the plane 2.4 A; and the O-H groups will extend 3.05 A from the center of the plane. The latter group would be the one which would cause the graphite oxide layers to expand to 6.1 A instead of 3.4 A for the original graphite. Now, if one assumes that the effective van der Waals radius of the carbon atom in graphite oxide is the same as it is in graphite, its effective radius

will be 1.71. If this is true, then the free space between carbon layers in graphite oxide will be 6.1 minus 3.4 A or 2.7 A. The van der Waals diameter of nitrogen is 3.0 A (61,p.189), which should be quite close to the effective diameter of  $\text{NH}_3$ . This assumption may be considered valid if one considers  $\text{NH}_3$  analogous to water. In the clays referred to above the effective diameter of water is approximately 2.6 to 2.8 A. This agrees quite well with 2.8 A, which is the van der Waals diameter of oxygen, which should be similar in effect to the nitrogen in  $\text{NH}_3$ .

The difference between the diameter of  $\text{NH}_3$  and the free space is approximately 0.3 A; the difference between 6.1 A and 6.65 A for the first plateau (sample 1-P58a) is 0.6 A, which is good agreement, considering the assumptions that were made. This means that essentially up to the first plateau,  $\text{NH}_3$  is being adsorbed between the carbon layers themselves with little expansion of c-spacing. This would also explain the small expansion of the c-spacing found by De Boer and Van Doorn above. If the oxygen from an ether linkage extends from the center of the carbon plane 2.4 A, then any  $\text{NH}_3$  molecule between the oxygen and the next carbon plane should expand the c-spacing to 7.1 A. This is quite close in agreement with the 7.25 A found

CT-12 BROWN Super

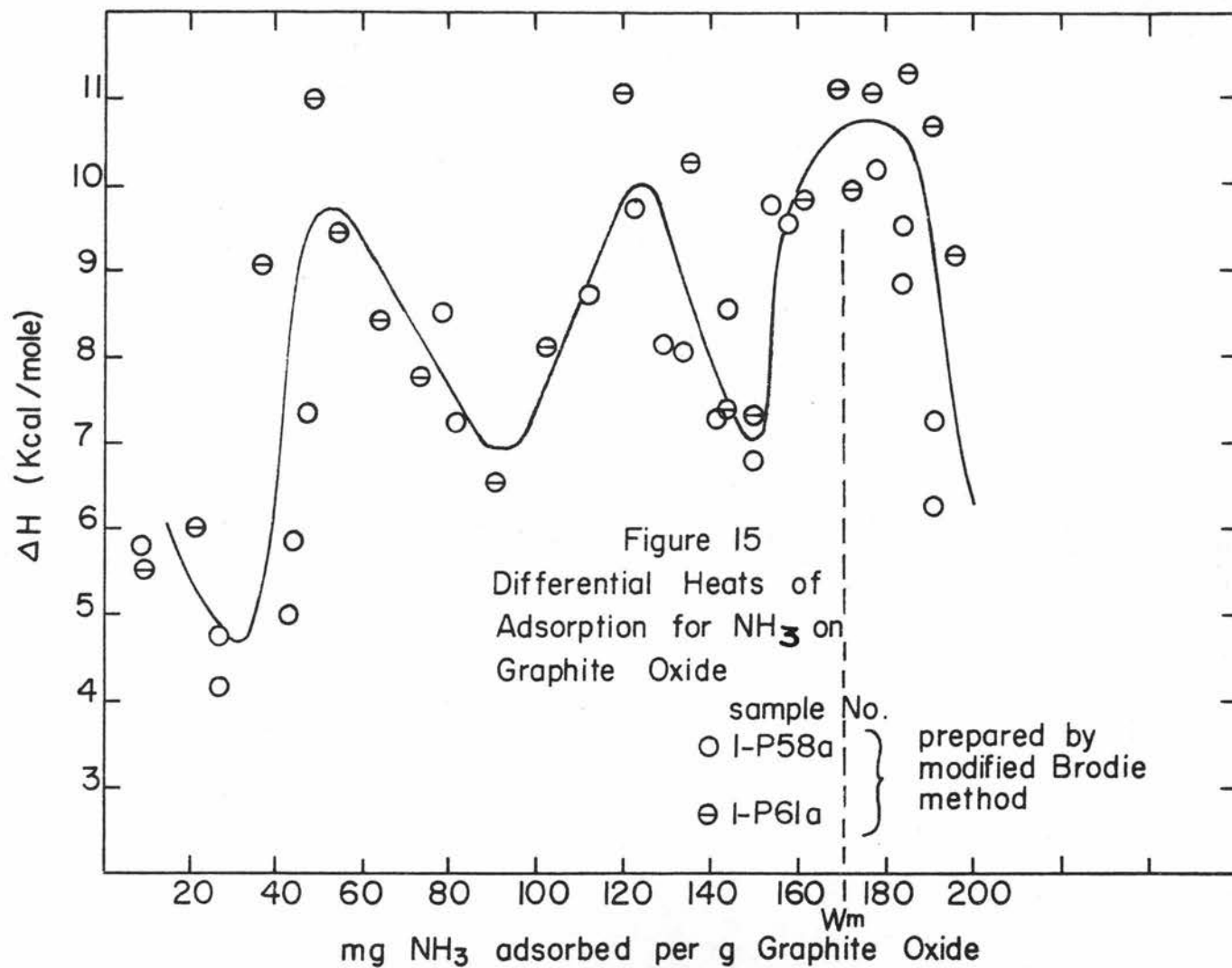
at the second plateau for sample 1-P58a. This information suggests that the initial adsorption of  $\text{NH}_3$  is in the open spaces surrounding the oxygens and O-H group, while the next addition of  $\text{NH}_3$  is between the ether groups and the carbon planes. If the 162 mg./g. of water found by De Boer and Van Doorn to be  $W_m$  corresponds to the 122 mg./g. of  $\text{NH}_3$  at the first plateau, this would mean that the difference between the water monolayer and the  $\text{NH}_3$  monolayer would be the area covered by the ether linkages in between the platelet. The difference between the area for  $\text{NH}_3$  at 122 mg./g. and at 175 mg./g. of graphite oxide is 245 m<sup>2</sup>/g. The difference between the area found from  $\text{NH}_3$  isotherms and those found from water is approximately 190 m<sup>2</sup>/G. which may be considered in fair agreement with the other difference.

One thing should be emphasized at this point, and that is the fact that the c-spacing measured in this experiment does not have to belong to the entire graphite oxide laminae. In fact, it probably belongs only to the crystalline part of the entire structure. Therefore, the mechanism proposed above would apply only to this portion of the structure.

### Heats of Adsorption

Discussion of error. The calorimetric heats of adsorption found are shown in Figure 15. The scattered points demonstrate poor reproducibility. This fact may be attributed to a number of reasons. One of the major difficulties was that the first 50 to 75 per cent of the adsorption took place in the first five minutes, while the rest of the adsorption was spread over the remaining hour and a half. This meant a large amount of heat was evolved at first, and considerably smaller amounts were given off toward the end of the determination. In fact, the last trace of  $\text{NH}_3$  adsorbed could not be detected with the calorimeter. This difficulty shows that, ideally, the calorimeter should be designed in order to accommodate an extremely long range of heats of adsorption. A calorimeter of this range is subject to many inherent errors.

There is also the possibility that the thermistors may have been unstable over the period of time involved in the determination. The thermistors were checked frequently and they showed seemingly good stability, although the check period was much shorter than the actual runs. As it was mentioned previously, error was introduced in the determination of the area under



the time-temperature curves by cutting out these graphs and weighing them because of the difference in the density of the paper. There is also an inherent error in the calculation of the heats of adsorption by the method of comparing the areas under the curves from the adsorption runs with those obtained from the calibration runs because the assumption is made that the rate of heat conduction is the same in both cases. This may not be true over relatively long periods of time. It is estimated that the total error is approximately  $\pm 7$  per cent.

Discussion of results. In spite of the wide deviation of points, three peaks may be observed in the graph. These peaks correspond quite well with the breaks in the curves shown in Figure 13 for the x-ray diffraction data with the exception of the first peak. This peak occurs a little before the first break; the other two peaks agree quite well.

There is no known case in the literature where the differential heats of adsorption show a similar pattern. There are some systems, such as the adsorption of water vapor on bovine serum albumin (1, p. 3980-3984) which show several peaks in the heat curve up to and including monolayer coverage. However, in the normal

case for heterogeneous systems, the initial heats are quite high as the more energetic sites are filled; then the values decrease continually with the possibility of another smaller maximum at or near the completion of a monolayer (59,p.51-53)(4,p.95-101). However, the nature of graphite oxide is quite complex and cannot be expected to comply with the more classical systems usually found in the literature.

The values for the heats of adsorption shown in Figure 15 include the heat of vaporization of  $\text{NH}_3$  (5.14 kcal.). As it was stated previously, the range of these values agree quite well with the range of isosteric heats calculated from the  $\text{NH}_3$  adsorption isobars. From this range one would surmise that the process is definitely one of physical adsorption; however, other factors indicate that this cannot be entirely true. There must be at least some hydrogen bonding as well as the salt formation found by infrared absorption.

The heats of adsorption were relatively low for the first uptake of  $\text{NH}_3$  by graphite oxide with some points even below the heat of vaporization of  $\text{NH}_3$ . Since normally the region should show high heat values, especially from any reaction with carboxyl groups on the edge of the lattice, this is an indication of some interaction requiring a considerable quantity of energy.

Slabaugh and Hatch (8,p.453-455) noticed the same phenomena with the isosteric heats of water vapor on graphite oxide. In their work, they found initially low isosteric heats with a rather sharp increase to a maximum heat value and then a steady decline until they were well below the initial heat values. They proposed that these first low values were due to the water gradually separating the layers and that the peak was due to adsorption of water on the more active sites exposed by separation of platelets.

The same mechanism could be proposed in this region for the adsorption of  $\text{NH}_3$  vapor. It is further proposed that the reason for these low values is that considerable energy is required to break hydrogen bonds and van der Waals attraction between the adjacent layers in graphite oxide. The heat required to rupture hydrogen bonds alone would range from 4.5 Kcal. for alcohol type groups to over 8 Kcal. for carboxylic acid groups (61,p.304-307). This would not conflict with the mechanism for adsorption proposed from X-ray data if this phenomena occurred primarily at the edges of the graphite oxide lattice. As it is, the X-ray diffraction curve in this region, especially for sample 1-P58a, shows little expansion in c-spacing, indicating that the major portion of the lattice is unaffected.

As with the isosteric heats from water vapor, the first maximum in Figure 15 could be attributed to adsorption of  $\text{NH}_3$  with the more active sites exposed by the initial adsorption because this peak occurs approximately in the region where the c-spacing of graphite oxide is increasing. As these sites become saturated and as further expansion takes place, the heat values would subsequently decrease as shown in the graph.

Further expansion would not necessarily require as great an amount of energy to pry the layers apart; therefore, the heat values would increase as more active sites were exposed, until a maximum is reached where the lamellar platelets are completely split apart. Then again, the heat would decrease as saturation of the active centers takes place. However, in the completed monolayer, lateral interaction (5, p. 746-754) and hydrogen bonding between  $\text{NH}_3$  molecules increase the total heat. As the second layer of  $\text{NH}_3$  is started, considerable energy would be required to spread the platelets, and the heats of adsorption would drop.

There are perhaps some discrepancies in mechanisms proposed above; however, it appears that a very complex sequence of events is involved, in which no single

explanation is justified. Other factors might be involved which have not been discussed. For example, there has been no reference made to the effects of any holes made in the lattice because of tautomerism or other broken bonds. These, of course, could possibly be placed in the category of active sites because of lateral interaction and hydrogen bonding within the confines of these openings. Another factor which was not discussed is the folding in the graphite oxide layers which have been detected by electron micrographs. A structure like this would require different degrees of energy, depending on the different degrees of folding.

#### Summary of Adsorption Mechanism

The heats of adsorption and X-ray data indicate the following mechanism for the adsorption. The initial uptake of  $\text{NH}_3$  occurs on the very active sites on the edges of the particles. Next, the  $\text{NH}_3$  is adsorbed between the carbon atoms in the two adjacent layers where it is attracted to sites on the face of the platelets. This involves the breaking of hydrogen bonds and the straightening of folded layers. The first molecules entering between the platelets would be ad-

sorbed by the most energetic sites. These molecules act as supports for the platelets like pillars in a building. As more  $\text{NH}_3$  molecules are adsorbed, they fill in the voids between the supporting molecules with relative ease, until all available space is filled. This available space would also include the capillaries or holes made by broken bonds.

As the pressure is increased, the  $\text{NH}_3$  enters between the oxygen and carbon atoms from adjacent graphite oxide layers. Here again, the first molecules act as supports, while the subsequent molecules fill in the voids as before. The adsorption of more  $\text{NH}_3$  involves the formation of a second layer, which requires considerable energy because of the formation of hydrogen bonds between the graphite oxide layers and the  $\text{NH}_3$  molecules.

The results found in this work tend to support the model for graphite oxide proposed by Ruess (Figure 1a). However, it does not give any direct evidence as to whether the carbon layers are planar or warped in structure. The tautomeric form shown in Figure 1b must not be discounted, but it is felt that this type is only a minor part of the over-all structure and is located principally in the regions near the edges of the platelets.

## FURTHER INVESTIGATION SUGGESTED BY THIS STUDY

Adsorption Studies

A number of new adsorption studies may be suggested at this time. It would be very interesting to study the adsorption of an acid anhydride such as  $\text{SO}_2$  and  $\text{CO}_2$  on graphite oxide, as well as the adsorption of amines and diamines of different chain lengths. Studies might be made on the adsorption of gases by graphite oxide in different stages of oxidation. Another interesting project in adsorption would be the study of the kinetics of adsorption. This would entail the use of a manostat on the adsorption system to maintain constant pressure.

Miscellaneous Studies

Polarography. Since the colloidal particles of graphite oxide are negatively charged and will migrate to the anode, it is possible that the system could be analyzed polarographically. This type of analysis should indicate the number of oxidizable groups on the compound. Of course, this study would depend on a constant diffusion rate of the graphite oxide; however, good results were obtained by Hallum and Drushel (32,

p.110-117) in work of this type on carbon blacks.

Ultra violet spectrophotometry. If graphite oxide contains enol groups, the neutralization of these groups should create a conjugated system ( $C=C-O^- Na^+$ ) which should absorb u-v radiation in the region of 200-350  $m\mu$ . Cursory examination of graphite oxide in basic solutions shows that there is absorption at 240 and 300  $m\mu$ . Further studies should be made to determine the intensity of this absorption versus pH and to determine the exact nature of the groups which absorb in this region.

Infrared spectrophotometry. A study of infrared absorption might be made on graphite oxide at different stages of oxidation. Further work could also be done on graphite oxide with adsorbed gases. There is also the possibility that if a sheet of graphite oxide could be made thin enough to be transparent to infrared radiation, then infrared studies could be made with adsorbed gases at various pressures in a special cell.

Heats of Immersion. There seems to be no reason that heats of immersion in liquid  $NH_3$  could not be found. A special calorimeter would have to be built in which dry-ice or a similar coolant would be necessary in order to keep  $NH_3$  in the liquid form. In such

a system it might be possible to measure the heat by the vapor pressure of  $\text{NH}_3$  over the liquid.

#### SUMMARY

Adsorption isotherms of  $\text{NH}_3$  on graphite oxide and graphite oxide salts were obtained at  $-45^\circ$  and  $-35^\circ$ . B.E.T. analyses of these isotherms indicated surface areas of 780-790  $\text{m}^2/\text{g}$ . for graphite oxide and 655  $\text{m}^2/\text{g}$ . for graphite oxide salts, which corresponded quite well with those found from the "point B" method.

Adsorption isobars were obtained, the shape of which indicated that the adsorption was physical in nature. This type of adsorption was supported by heats of adsorption obtained from the isobars and by direct calorimetric measurement.

Infrared absorption spectra was obtained on graphite oxide with and without adsorbed  $\text{NH}_3$ . The results indicated the formation of  $\text{NH}_4^+$  ions and hydrogen bonding on the adsorption of  $\text{NH}_3$  on the oxide.

X-ray diffraction data was obtained for graphite oxide with various quantities of adsorbed  $\text{NH}_3$ . Two plateaus were obtained in the c-spacing up to the formation of a monolayer. A mechanism was proposed in an attempt to explain this phenomenon.

The heats of adsorption were measured calorimetrically. The heats of adsorption curve had three similar maxima. An attempt was made to correlate these maxima with the data obtained from x-ray diffraction. An over-all adsorption mechanism was postulated.

## BIBLIOGRAPHY

1. Amberg, C.H. Heats of adsorption of water vapor on bovine serum albumin. *Journal of the American Chemical Society* 79:3980-3984. 1952.
2. Balbiano, M.L. Etude sur l' acid graphitique. *Bulletin de la société Chimique de France* 19: 191-203. 1873.
3. Beckett, R.J. and R.C. Croft. The structure of graphite oxide. *Journal of Physical Chemistry* 56:929-935. 1952.
4. Beebe, R.A. et al. *Journal of the American Chemical Society* 69:95-101. 1947.
5. Beebe, R.A. and R.M. Dell. Heats of Adsorption of polar molecules on carbon surfaces. I. Sulfur dioxide. *Journal of Physical Chemistry* 59:746-754. 1955.
6. Beebe, R.A., B. Millard and J. Cynarski. Heats of adsorption of nitrogen and argon on porous and on non-porous carbon adsorbents at  $-195^{\circ}$ . *Journal of the American Chemical Society* 75:839-845. 1953.
7. Boer, J.H. de and A.B.C. van Doorn. Graphite oxide. I. The formula and specific volumes of the hydrates. *Koninklijke Nederlandse Akademie van Wetenschappen B*, 57:181-191. 1954.
8. Boer, J.H. de and A.B.C. van Doorn. Graphite oxide. II. The oxidation of several types of graphite. *Koninklijke Nederlandse Akademie van Wetenschappen B*, 61:12-16. 1958.
9. Boer, J.H. de and A.B.C. van Doorn. Graphite oxide. III. The thermal decomposition of graphite oxide. *Koninklijke Nederlands Akademie van Wetenschappen B*, 61:17-21. 1958.
10. Boer, J.H. de and A.B.C. van Doorn. Graphite oxide. IV. Some chemical properties. *Koninklijke Nederlands Akademie van Wetenschappen B*, 61:160-169. 1958.

11. Boer, J.H. de, and A.B.C. Van Doorn. Graphite oxide. V. The sorption of water. Koninklijke Nederlandse Akademie van Wetenschappen B, 61:242-252. 1955.
12. Bottomley, G.A. and J.G. Blackman. Graphitic acid from aromatic compounds by peroxide treatment. Nature 171:620. 1953.
13. Brodie, B.C. On the atomic weight of carbon. Philosophical transactions of the Royal Society of London. 149:249-259. 1859.
14. Brown, Bruce K. Graphitic oxide as a depolarizer in the Le Clanche cell. Transactions of the American Electrochemical Society 33:113-118. 1928.
15. Brown, Bruce K. and Oliver Storey. Electrochemical production of graphitic oxide. Transactions of the American Electrochemical Society 53:129-147. 1928.
16. Brunauer, Stephen, and Paul H. Emmett. The use of low temperature van der Waals adsorption isotherms in determining the surface area of iron synthetic ammonia catalysts. Journal of the American Chemical Society 59:1553-1564. 1937.
17. Brunauer, Stephen, and Paul H. Emmett. The use of low temperature van der Waals adsorption isotherms in determining the surface areas of various adsorbents. Journal of the American Chemical Society 59:2682-2689. 1937.
18. Brunauer, Stephen, Paul H. Emmett and Edward Teller. Adsorption of gases in multimolecular layers. Journal of the American Chemical Society 60:309-319. 1938.
19. Cano-Ruiz, J. and Douglas M.C. MacEwan. Interlamellar organic complexes of graphite oxide: A preliminary study. Tercera Reunion Internacional Sobre Reactividad De Los Solidos, April, 1956, p. 227-242.
20. Carter, H.H., L. de V. Moulds and H.L. Riley. The nature of the solid carbon-oxygen complex. I. The oxidative action of graphitic oxide and active carbon plus oxygen on some aromatic amines. Journal of the Chemical Society 1305-1312. 1937.

21. Charpy, M. Georges. Sur la formation de l'oxyde graphitique et la definition du graphite. Comptes Rendus des Seances de l'Academie des Science 148: 920-923, 1909.
22. Clauss, Alexander et al. Untersuchungen zur Struktur des Graphitoxys. Zeitschrift für Anorganische und Allgemeine Chemie 291:205-220. 1957.
23. Clauss, Alexander und Ulrich Hofmann. Graphitoxyd-Membranen zur Messung des Wasserdampf-Partialdruckes. Angewandte Chemie 68:522. 1956.
24. Cornet, I. Sorption of  $\text{NH}_3$  on montmorillonite clay. Journal of Chemical Physics 11:217-226. 1943.
25. Derksen, J.C. and J.R. Katz. Untersuchungen über die intramicellare Quellung der Graphitsäure. Recueil des travaux Chimiques des Pays-Bas 53: 652-669. 1934.
26. Dresel, E.M. Calorimeters and calorimetric heats of adsorption. 1953. 13 p. (Great Britain. Atomic Energy Research Establishment. A.E.R.E. C/R 1105).
27. Eischens, R.P., S.A. Francis and W.A. Pliskin. Effect of surface coverage on the spectra of chemisorbed  $\text{CO}$ . Journal of Physical Chemistry 60:194-201. 1956.
28. Emmett, Paul H. Multilayer adsorption equations. Journal of the American Chemical Society 68:1784-1789. 1946.
29. Foss, John G. and Hoyd H. Reyerson. The sorption of water vapor by lyophilized ribonuclease. Journal of Physical Chemistry 62:1214-1216. 1958.
30. Franklin, Rosalind E. Le role de l'eau dans la structure de l'acide graphitique. Journal de Chemie Physique C26:50.
31. Hadzi, D. and Novak, A. Infrared spectra of graphitic oxide. Transactions of the Faraday Society 51:1614-1620. 1955.
32. Hallum, Jules V. and Harry V. Drushel. The organic nature of carbon black surfaces. Journal of Physical Chemistry 62:110-117. 1958.

33. Halsey, George and Hugh S. Taylor. The adsorption of hydrogen on tungsten powders. *Journal of Chemical Physics* 15:624-630. 1947.
34. Hamdi, H. Die Elektrolyt-Koagulation des Graphit-oxyds. *Kolloid-Zeitschrift* 128:22-26. 1952.
35. Hamdi, H. Zur Kenntnis der Kolloidchemischen Eigenschaften des Humus. *Kolloid-Beihefte* 54:554-634. 1943.
36. Harkin, William D. and George Jura. Surface of solids. X. Extension of the attractive energy of a solid into an adjacent liquid or film, the decrease of energy with distance, and the thickness of films. *Journal of the American Chemical Society* 66:919-927. 1944.
37. Harkins, William and George Jura. Surface of solids. XII. An absolute method for the determination of the area of a finely divided crystalline solid. *Journal of the American Chemical Society* 66:1362-1366. 1944.
38. Harkins, William D. and George Jura. Surfaces of Solids. XIII. A vapor adsorption method for the determination of the area of a solid without assumption of a molecular area, and the area occupied by nitrogen and other molecules on the surface of a solid. *Journal of the American Chemical Society* 66:1366-1373. 1944.
39. Hatch, Conrad V. Thermodynamic characterization of graphitic oxide surfaces. Ph.D. Thesis. Corvallis, Oregon State College, 1960. 97 numb. leaves.
40. Hofmann, Ulrich. Über Graphitsäure und die bei ihrer Zersetzung entstehenden Kohlenstoffarten. *Berichte der Deutschen Chemischen Gesellschaft*. 61:435-441. 1928.
41. Hofmann, Ulrich. Röntgenoskopie lamellardisperser Systeme. *Kolloid-Zeitschrift* 69:351-357. 1934.
42. Hofmann, Ulrich. Über die Formel der Graphitsäure. *Kolloid-Zeitschrift*. 104:112-114. 1943.

43. Hofmann, Ulrich and Alfred Frenzel. Permutoid reactions of graphite. Zeitschrift für Elektrochemie 37:613-618. 1931. (Abstracted in Chemical Abstracts 26:352,6. 1932)
44. Hofmann, Ulrich and Alfred Frenzel. Quellung von Graphit und die Bildung von Graphit säure. Berichte der Deutschen Chemischen Gesellschaft 63:1248-1262. 1930.
45. Hofmann, Ulrich, Alfred Frenzel and E. Csalan. Die Konstitution der Graphitsäure und ihre Reactionen. Annalen der Chemie 510:1-41. 1934.
46. Hofmann, Ulrich and R. Holst. Über die Säurenatur und die Methylierung von Graphitoxyd. Berichte der Deutschen Chemischen Gesellschaft 72:754-771. 1939.
47. Hofmann, Ulrich and Ernest König. Untersuchungen über Graphitoxyd. Zeitschrift für anorganische und Allgemeine Chemie 234:311-336. 1937.
48. Hornig, Donald F. The vibrational spectra of molecules and complex ions in crystals. I. General Theory. Journal of Chemical Physics 16:1063-1076. 1948.
49. Hummers, William S. Jr. Preparation of graphitic acid. U.S. patent 2,398,878. July 9, 1957.
50. Hummers, Wm. S. Jr. and Richard E. Offeman. Preparation of graphitic oxide. Journal of the American Chemical Society 80:1339. 1958.
51. Joyner, L.G. and Paul H. Emmett. Differential heats of adsorption of nitrogen on carbon blacks. Journal of the American Chemical Society 70:2353-2359. 1948.
52. Kohlschutter, V. and P. Haenni. Zur Kenntnis des graphitischen Kohlenstoffs und der Graphitsäure. Zeitschrift für Anorganische und Allgemeine Chemie 105:121-144. 1919.
53. Langmuir, Irving. The adsorption of gases on plane surfaces of glass, mica and platinum. Journal of the American Chemical Society 40:1361-1403. 1918.

54. Lippincott, E.R., F.E. Welsh and C.F. Weir. Microtechnique for infrared study of solids using diamonds and sapphires as cell material. *Analytical Chemistry* 33:137-143. 1961.
55. MacEwan, D.M.C., J. Cano-Ruiz and F. Aragon. La sorcion interlaminar en acido grafítico y montmorillonita. *Anales de la Real Sociedad Espanola de Fisica y Quimica*. 55 B:677-682. 1959.
56. Maire, Jacques. Reaction du melange de Brodie avec les carbones graphitisables et non graphitisables. *Comptes Rendes des Seances de l'Academie des Sciences* 232:61-63. 1951.
57. Mapes, J.E. and R.P. Eischens. The infrared spectra of ammonia chemisorbed on cracking catalysts. *Journal of Physical Chemistry* 58:1059-1062. 1954.
58. Matuyama, Eitaro. Pyrolysis of graphitic acid. *Journal of Physical Chemistry* 58:215-219. 1954.
59. Mooi, John, Conway Pierce and R. Nelson Smith. Heats and entropies of adsorption on a homogeneous carbon surface. *Journal of Physical Chemistry* 27th National Colloid Symposium 57:51-53. 1953.
60. Pallman, H. Dispersoid chemische Probleme in der Humusforechung. *Kolloid-Zeitschrift* 101:72-81. 1942.
61. Pauling, Linus. Nature of the chemical bond. 2d ed. Ithaca, N.Y., Cornell University Press, 1945. 450 p.
62. Pliskin, W.A. and R.P. Eischens. The effect of using the pressed salt technique to obtain the spectrum of chemisorbed ammonia. *Journal of Physical Chemistry* 59:1156-1159. 1955.
63. Riley, H.R. Laminar Compounds of carbon. *Fuel in Science and Practice* 24:43-56. 1954.
64. Ruess, Gerhard. Uber das Graphithydroxyd (Graphitoxyd). *Monatshefte fur Chemie* 76:381-417. 1947.
65. Ruess, Gerhard. Zur Formel des Graphitoxys. *Kolloid-Zeitschrift* 110:17-26. 1945.

66. Siderov, A.N. Infrared-adsorption spectra of gaseous organic compounds on microporous glass. Doklady Akademii Nauk S.S.S.R. 95:1235-1238. 1954. (Abstracted in Chemical Abstracts 49:8703a. 1955)
67. Slabaugh, W.H. and Conrad V. Hatch. Graphitic oxide and water: Heats of immersion and heats of adsorption. Journal of Chemical and Engineering Data 5:453-455. 1960.
68. Staudenmaier, L. Verfahren zur Darstellung der Graphitsäure. Berichte der Deutschen Chemischen Gesellschaft 31:1481-1487. 1898.
69. Svatos, G.F., Columba Curran and J.V. Quagliano. Infrared adsorption spectra for inorganic coordination complexes. V. The N-H stretching vibration in coordination compounds. Journal of the American Chemical Society 77:6159-6163. 1955.
70. Thiele, Heinrich. Biologischer Abbau der Graphitsäure. Die Naturwissenschaften 34:218. 1947.
71. Thiele, Heinrich. Die Mizellarstruktur der Graphitsäure. Kolloid-Zeitschrift 56:129-138. 1931.
72. Thiele, Heinrich. Graphit und Graphitsäure. Zeitschrift für Anorganische und Allgemeine Chemie 190: 145-160. 1930.
73. Thiele, Heinrich. Über Ionotropie. Kolloid-Zeitschrift 115:167-168. 1949.
74. Thiele, Heinrich. Über Salzbildung und Basenaustausch der Graphitsäure. Kolloid-Zeitschrift 80:1-20. 1937.
75. Thiele, Heinrich and Heinrich Micke. Über Ionotropie. Einfluss der Mizellen. Kolloid-Zeitschrift 117: 144-153. 1950.
76. Trapnell, B.M.W. Chemisorption. New York, Academic Press Inc., 1955. 265 p.
77. Wagner, E.L. and D.F. Hornig. The vibrational spectra of molecules and complex ions in crystals. III. Ammonium chloride and deuterio-ammonium chloride. Journal of Chemical Physics 18:296-304. 1950.

78. Weiss, Joseph. Fluorescence and oxidation in conjugated ring systems. *Nature* 145:744-745. 1940.
79. Weisser, Harry Boyer. A textbook of colloid chemistry. 2d ed. New York, Wiley. 1949. 444 p.
80. Yates, D.C.J., N. Sheppard and C.L. Angell. Infrared spectrum of ammonia adsorbed on porous silica glass. *Journal of Chemical Physics* 23:1980-1981. 1955.
81. Zettlemyer, A.C., J.J. Chessick and Amir Chand. Sorption by Organic Substances. II. Effect of functional groups on ammonia sorption. *Journal of Physical Chemistry* 59:375-378. 1955.
82. Zettlemyer, A.C., G.J. Young and J.J. Chessick. Studies of the surface chemistry of silicate minerals. III. Heats of immersion of bentonite in water. *Journal of Physical Chemistry* 59:962-966. 1955.